UNIVERSITY OF CALIFORNIA
RIVERSIDE

WALLFLOWER (WFL): A LRR-RLK, Simultaneously Localizes to Opposite Sides of Root Hair Cells and Functions to Position Hairs

A Dissertation submitted in partial satisfaction
of the requirements for the degree of

Doctor of Philosophy

in

Plant Biology

by

Jessica Nichole Toth

March 2021

Dissertation Committee:
Dr. Jaimie Van Norman, Chairperson
Dr. Patricia Springer
Dr. Carolyn Rasmussen

The Dissertation of Jessica Nichole Toth is approved by:

_____

_____

_____

Committee Chairperson

University of California, Riverside

ACKNOWLEDGEMENTS

Initial Research Evaluation Committee:

Jaimie M. Van Norman

Linda Walling

Carolyn Rasmussen

Qualifying Exam Committee:

Carolyn Rasmussen

Patricia Springer

Meng Chen

Linda Walling

Morris Maduro

Dissertation Committee:

Jaimie M. Van Norman

Patricia Springer

Carolyn Rasmussen

Funding:

NSF-GRFP #DGE-1326120 (J.N.T.)

NSF CAREER (J.M.V.) #1751385

USDA-NIFA-CA-R-BPS-5156-H (J.M.V.)

Note from Author:

Many thanks and all of my love to my family, friends, and colleagues – who never let me go over or under it, but encouraged me to go through it.

ABSTRACT OF THE DISSERTATION

WALLFLOWER (WFL): A LRR-RLK, Simultaneously Localizes to Opposite Sides of Root Hair Cells and Functions to Position Hairs

by

Jessica Nichole Toth

Doctor of Philosophy, Graduate Program in Plant Biology
University of California, Riverside, March 2021
Dr. Jaimie M. Van Norman, Chairperson

Polarized cells are frequently partitioned into subdomains with unique features or functions. As plant cells are surrounded by rigid walls, polarized cell shape and protein polarity in the plasma membrane are particularly important for normal physiology and development. Here we identify and characterize WALLFLOWER (WFL), a transmembrane receptor kinase that is asymmetrically distributed to the inner face of epidermal cells. In epidermal hair (H) cells in the elongation and differentiation zones, WFL exhibits a dual polar localization, accumulating at the inner domain as well as at the root hair initiation domain (RHID). While WFL localization to the inner polar domain remains constant regardless of cell identity, its localization is affected by deletion of the intracellular domains. Polar localization of truncated WFL varies depending on cell identity indicating the WFL intracellular domains are important for informing cell type-specific positional information. Additionally, we observe that polar accumulation of WFL at specific

plasma membrane domains is achieved and maintained by constant *de novo* protein secretion via a Brefeldin A sensitive endomembrane trafficking pathway. While *wfl* mutants don't have a detectable abnormal phenotype, overexpression of *WFL* leads to a downward shift in root hair (RH) position. However, RH position is unaffected upon deletion of WFL intracellular domains, indicating that the kinase domain is required to inform RH position. Additionally, we find that roots overexpressing WFL-GFP are also sensitive to mechanical stress and prone to cell damage. However, this phenotype can be alleviated by cell wall rigidification or maintaining stable osmotic conditions. These observations, together with the shifted RH phenotype, suggest that WFL may have a role in coordinating cell wall modification with cellular expansion during RH development. We propose WFL participates in a signaling pathway that links cues from the inner cell layers of the root with polar growth at the epidermal surface, informing RH position.

TABLE OF CONTENTS

LIST OF FIGURES

LIST OF TABLES

CHAPTER ONE: Cell polarity influences a diverse suite of developmental processes in the *Arabidopsis* root

ABSTRACT

In plants, cells are fixed in place due to a rigid cell wall and therefore, cell polarity and directional signaling are important for normal physiology and development. Cell polarity can be described as an asymmetry in the localization of subcellular constituents and/or cell morphology. Polar localization of proteins to specific plasma membrane domains impacts protein function, activity, and stability, and has a direct influence on intercellular communication, development, and environmental interactions. Establishment and maintenance of protein polar localization is influenced by multiple factors including endomembrane trafficking, cell- and organ-specific cues, and/or specific protein domains. In this chapter, we discuss the *Arabidopsis* root as a model system for studying various aspects of cell polarity and development. We address how polarly localized proteins achieve and maintain polar accumualtion to specific plasma membrane domains. Additionally, we discuss how polar localization to specific plasma membrane domains is often linked to biological function in development.

INTRODUCTION

Cell polarity in plant cells

In multicellular eukaryotic organisms, cells are frequently partitioned into subdomains with unique features or functions and can therefore be described as polarized. Cell polarity can be defined as asymmetry in the localization of subcellular constituents and proteins and/or in cell morphology. One of the primary ways that cell polarity is achieved is through preferential accumulation of proteins at specific subcellular locations. Partitioning of the plasma membrane (PM) can impact protein function, activity, and stability; therefore, it has tremendous regulatory potential in intercellular communication, development, and environmental interactions (Łangowski et al., 2016; Nakamura & Grebe, 2018; Van Norman, 2016). Because plant cells are fixed in place due to the cell wall, polarized protein accumulation is required for diverse physiological and developmental processes, such as asymmetric cell division, localized cell growth, long- and short-range signal transduction, and directional transport(Breda et al., 2017; Petrásek & Friml, 2009; Takano et al., 2010). A fundamental question in cell and developmental biology is: how is cell polarity established and maintained and what are its functional consequences? This question is often addressed using the *Arabidopsis* root where the consequences of cellular asymmetries in cell division, differentiation, and polarity are elegantly displayed; making the root an excellent model to investigate links between cell polarity and development.

The *Arabidopsis* root and hair: a model system in cell polarity and development

In the *Arabidopsis* root, cellular organization is largely invariant and developmental events are predictable, making it an excellent system to study cellular or organ function and link it to various aspects of cell polarity. The root is cylindrical in shape with cells forming concentric layers around the central vascular tissues (Figure 1.1A) and individual cells arranged in files that extend from the root tip shootward (Figure 1.1B and D, Dolan et al., 1993). In the longitudinal axis the root is divided into three developmental zones: the meristematic, elongation, and differentiation zones where cells divide, expand, or mature, respectively (Figure 1.1D, Benfey & Scheres, 2000). These organizational features allow for straightforward analysis of protein localization and developmental phenotypes in the root.

In individual root cells, the PM is typically partitioned into four distinct polar domains (Figure 1.2A). Proteins that polarly localize to these domains are described as shootward or rootward localized (Figure 1.2A and C) when they accumulate toward the shoot or root apices, respectively. Laterally localized proteins have inner or outer polar localization when they accumulate towards or away from the root vasculature, respectively (Nakamura & Grebe, 2018). However, polarized proteins can also be localized to smaller regions than an entire cell face. For example, development of root epidermal hair cells is an

excellent model of how polar protein localization and polar cell morphology are achieved and maintained during development.

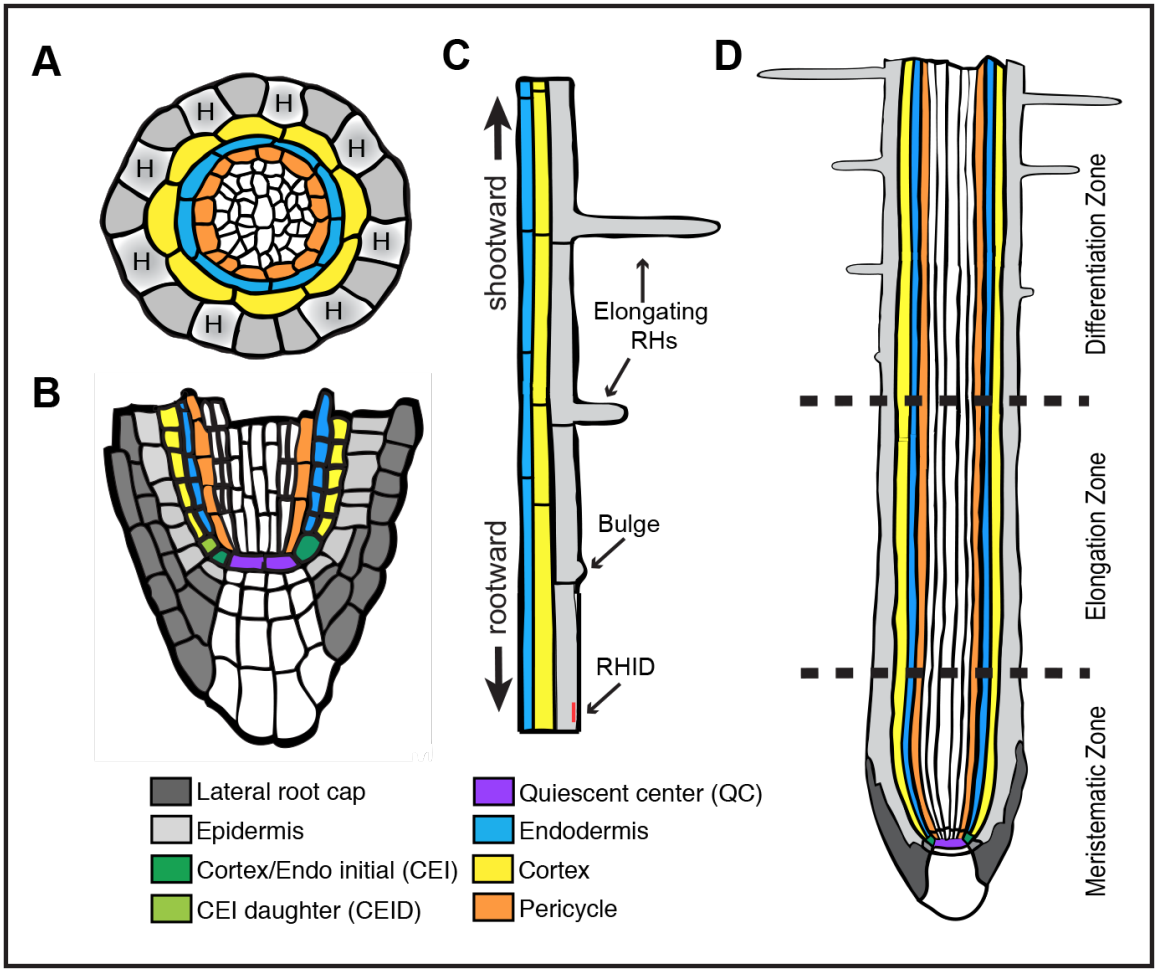

Figure 1.1: Root cellular organization, RH development, and root developmental zones. Schematic sections of the *Arabidopsis thaliana* root tip in the (A) transverse and (B) median longitudinal. (C) Schematic of RH development in the longitudinal axis from RHID (red line), to bulge, to fully elongated RH. (D) Median longitudinal schematic of the root tip showing developmental zones. Abbreviations: RHID, root hair initiation domain; RH, root hair; H, hair cell.

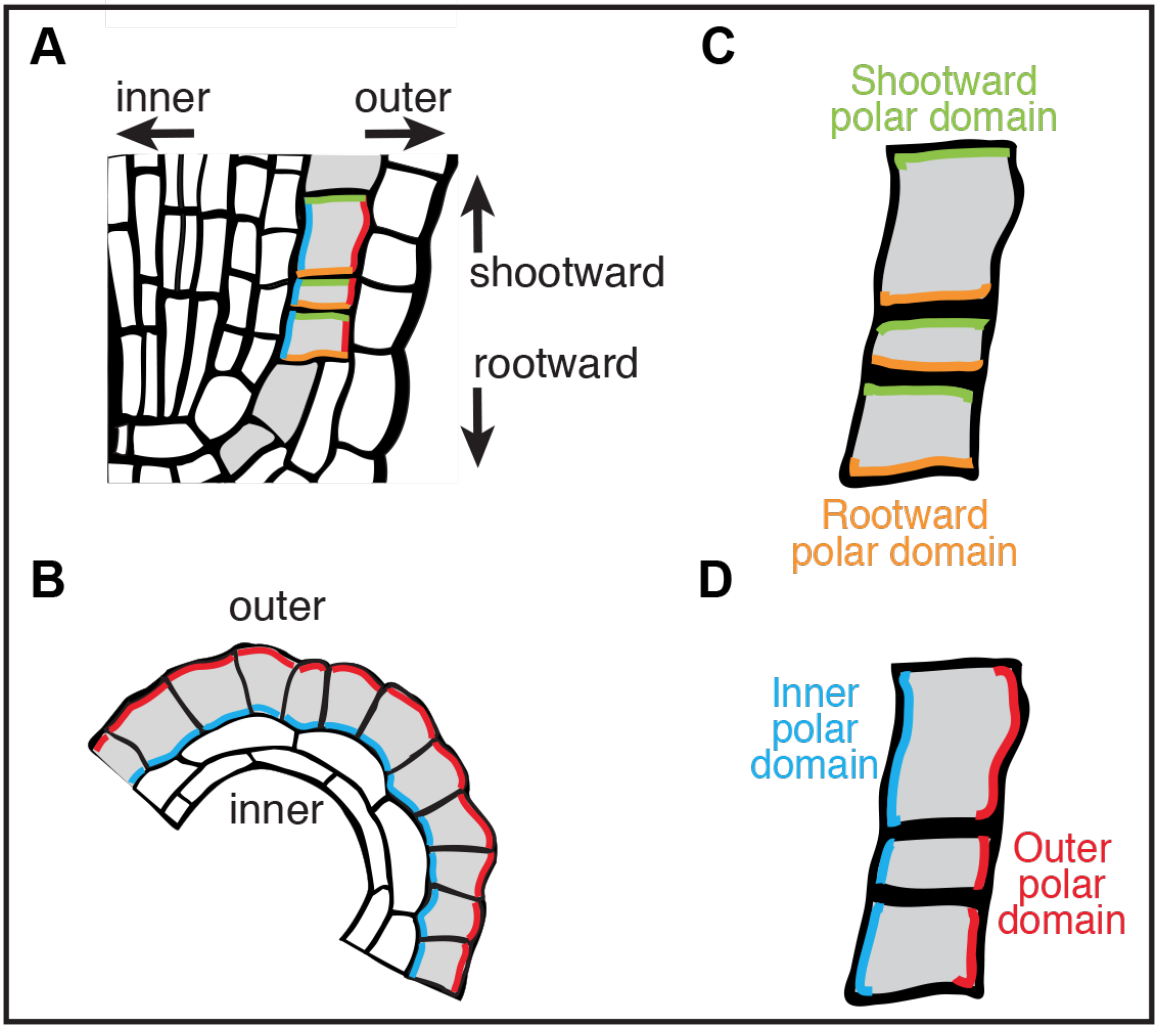

Figure 1.2: Plasma membrane polar domains in root cells. (A and B) Schematic sections of the *Arabidopsis thaliana* root tip showing plasma membrane domains in the (A) median longitudinal and (B) transverse. (C and D) Schematic sections of individual cells in the median longitudinal showing more detail of the (C) shootward (green)/rootward (orange) and (D) inner (blue)/outer (red) polar domains.

In the root epidermis, cell identity is position dependent relative to the underlying cortical cells. When positioned over the junction of two cortex cells, epidermal cells acquire hair (H) cell identity whereas, an epidermal cell positioned over a single cortex cell will have non hair (NH) cell identity (Figure 1.1A, Costa &Dolan,

2000; Dolan et al., 1993). In the differentiation zone, epidermal cells with H cell identity will form long tubular extensions called root hairs (RHs) (Figure 1.1C and D). RHs function in plant anchorage and increase the total surface area of the root allowing for maximal water and nutrient uptake from the soil (Grierson et al., 2014). Additionally, RHs are a dramatic example of morphological polarity in plant cells and are therefore, an ideal system for studying various aspects of cell polarity (Schiefelbein & Somerville, 1990).

RH development occurs in two stages: (1) initiation and (2) tip growth through targeted secretion. Initiation of RHs requires the establishment of an additional polar domain within H cells, the RH initiation domain (RHID, Figure 1.1C). In *Arabidopsis*, positioning of the RHID in the longitudinal axis is uniformly confined to a very small region on the outer face of epidermal H cells, approximately 10 μm from the rootward edge (Figure 1.1C, Grierson et al., 2014). Establishment of the RHID requires polar localization of proteins to this specific region at the outer face and toward the rootward end of H cells. One of the first proteins to arrive at the RHID is ROP GUANINE NUCLEOTIDE EXCHANGE FACTOR 3 (GEF3) followed by recruitment of RHO-RELATED PROTEIN FROM PLANTS (ROP2, Denninger et al., 2019). This leads to softening of the cell wall at the RHID and local formation of a bulge on the H cell surface that increases in size and becomes more defined (Figure 1.1C, Grierson et al., 2014).

After the RHID is established, a dome-shaped outgrowth, or bulge, is formed and leads to a series of events including cell wall acidification and loosening that facilitates the onset of RH elongation through a process known as tip growth (Gilroy and Jones 2000). Intensive polarized secretion of cellular and cell wall materials to the RHID lead to bulge formation and tip growth in H cells. Many proteins show higher accumulation at the growing tip of RHs; some of these proteins may be caught up in the default secretion scheme of RH elongation, but others, including many involved in signaling, are specifically localized to this region because they have important functions in maintaining tip growth and cell wall integrity. For example, FERONIA (FER), a member of the *Catharanthus roseus* RECEPTOR-LIKE KINASE 1-LIKE (CrRLK1) subfamily of putative cell wall sensors, is polarly localized to the RHID and bulge during RH development (Zhu et al., 2020). FER forms a complex with ROPs and GEFs and functions in RH tip growth through accumulation of reactive oxygen species (ROS) at the RH tip (Duan et al., 2010; Huang et al., 2013). ERULUS (ERU), another CrRLK1-related receptor, preferentially accumulates at the growing RH tip where it acts as a cell wall sensor protein and functions to inhibit pectin methylesterase activity during RH growth (Kwon et al., 2018; Schoenaers et al., 2018). These observations suggest that polar localization of proteins to specific PM domains can be linked to their biological function.

Polar localization to specific PM domains is often linked to biological function

In plants, the majority of characterized polarized transmembrane proteins are transporters whose localization is intuitively linked to their function in directional transport. The transporters of the plant hormone auxin have well characterized polar localization with efflux transporters, the PIN-FORMED (PIN) proteins, and influx carriers, AUXIN RESISTANT 1/LIKE AUXIN RESISTANT1 (AUX1/LAX) proteins, localized to the rootward and/or shootward polar domains to drive directional transport of auxin (Laskowski et al., 2008; Petrásek & Friml, 2009; Swarup et al., 2001; Wisniewska et al., 2006). Directional movement of auxin from cell-to-cell mediates many developmental processes including cell division and elongation and is required for continuous root growth (Baster & Friml, 2014; Habets & Offringa, 2014). At the lateral faces of root cells, boron transporters, such as NODULIN26-LIKE INTRINSIC PROTEIN 5;1 (NIP5;1) and REQUIRES HIGH BORON 1 (BOR1) are oriented to the outer and inner polar domains, respectively, and facilitate Boron uptake from the soil and transport in the root (Takano et al., 2002, 2006, 2010).

Polarized protein localization in root cells extends beyond transporters to a range of other proteins, including those involved in intracellular signaling and development. In the meristematic zone, a leucine-rich repeat receptor-like kinase (LRR-RLK) called INFLORESCENCE AND ROOT APICES RECEPTOR KINASE

(IRK) is localized to the outer polar domain in the endodermis and *irk* mutants have altered cell divisions in that cell type (Campos et al., 2020). Additionally, BREVIS RADIX (BRX) and OCTOPUS (OPS), rootward and shootward localized, respectively, are required for phloem development (Breda et al., 2017; Truernit et al., 2012). In the differentiation zone, SCHENGEN1 (SGN1), a receptor-like cytoplasmic kinase and SGN3/GASSHO1, an LRR-RLK, are polarly localized in maturing root endodermal cells and required for Casparian strip formation (Alassimone et al., 2016; Pfister et al., 2014). Additionally, LRR-RLKs, MOUSTACHES (MUS) and MOUSTACHES-LIKE (MUL), localize to the rootward polar domain and are necessary for normal lateral root formation (Xun et al., 2020). While the physiological imperative for directional transport is clear, the necessity for position-specific signal perception is less apparent. Indeed, the function of BRX and OPS in phloem development does not depend on their specific polar localization (Breda et al., 2017). Whether these polarized transmembrane or membrane-associated proteins perceive extracellular signals, act as scaffolds, or plasma membrane-delineated boundaries for position-dependent developmental processes remains to be fully understood.

Multiple factors inform establishment and maintenance of protein polarity at the PM

One of the primary questions with regard to cell polarity is: how is polar localization of proteins established and maintained. There is evidence that polarized proteins can be directed through multiple endomembrane pathways to specific PM domains. However, the underlying mechanisms and the diversity of these mechanisms for different types of proteins remains poorly understood. Localization of the PIN proteins is the most well characterized, and it is known that maintenance of PIN polarity occurs by hyper-polar secretion of *de novo* synthesized protein, constant cycles of endocytosis and recycling, and restriction of lateral diffusion (Naramoto, 2017). Additionally, PIN polarity can be disrupted by the endocytic inhibitor, Brefeldin A (BFA). In contrast, polar localization of the receptor kinases IRK and KINASE ON THE INNERSIDE (KOIN) is primarily driven by polar secretion of *de novo* protein. Additionally, IRK polar secretion is sensitive to BFA and that of KOIN is largely resistant, but importantly, polar localization of IRK and KOIN is unaltered upon treatment with BFA (Rodriguez-Furlán et al. 2021). This indicates the mechanisms underlying establishment and maintenance of polarity for receptor kinases is distinct from the paradigm established for transporters like the PINs. Furthermore, this suggests that multiple trafficking pathways inform and direct polar localization of different proteins to different PM domains and highlights that polar localization of plant proteins is complex and incompletely understood.

Polar localization of proteins to specific PM domains in different tissue types implies that positional information can be derived from cell and/organ level cues. Polar accumulation of full length IRK changes depending on cell type, suggesting its localization is directed by local cues from adjacent cells (Campos et al., 2020). In contrast, lateral localization of KOIN stays the same regardless of cell identity (Rodriguez-Furlán et al. 2021), suggesting that, as proposed for some nutrient transporters (Alassimone et al., 2010), its localization is informed by an organ-level cue originating from the stele. Additionally, localization of different proteins to distinct polar domains suggests that there are also protein specific domains or motifs required for correct polar localization. For receptor kinases, it has been found that specific protein domains differentially inform polar localization. KOIN is polarly localized to the inner polar domains of root endodermal cells and upon removal of its intracellular domains, becomes nonpolar, whereas, polar localization of IRK does not change when its intracellular domains are removed (Rodriguez-Furlán et al. 2021). These diverse localization outcomes, indicate that a variety of factors govern polar accumulation of transmembrane proteins in plant cells and the underlying mechanisms remain an area of intense study.

Polar localization of WALLFLOWER (WFL) is linked to its function in RH positioning

To gain additional insights into how cell polarity and root development are linked, we investigated the localization and function of WALLFLOWER (WFL), a LRR-RLK with dual polar localization in root epidermal H cells. We show that in H cells, WFL localizes simultaneously to the inner polar domain as well as the RHID and bulges within the outer polar domain. Our results show that WFL polar localization is mainly achieved by *de novo* protein synthesis and secretion through a BFA-dependent mechanism and that inner polar localization remains consistent regardless of cell identity. However, WFL asymmetric localization is disrupted upon removal of its intracellular domains, resulting in mislocalization to the outer polar domain of H cells and exclusion from RHIDs and RH bulges. In contrast to full length WFL, localization of truncated WFL varies with cell type, indicating that WFL intracellular domains inform cell type-specific localization. While *wfl* mutants have no detectable abnormal phenotype, we observe that RH position is shifted downward in H cells upon WFL overexpression. Furthermore, RH position is unaffected in roots expressing the truncated version of WFL, indicating that its intracellular domains are required to inform RH position. Additionally, we find that WFL overexpression results in roots that are sensitive to mechanical and osmotic stress and are therefore prone to cellular damage. However, the severity of these phenotypes can be reduced by either cell wall rigidification or maintaining stable osmotic conditions. Thus, we propose that

WFL intracellular domains are necessary to link cues from the inner cell layers of the root to inform its localization and function in RH positioning.

Research Outline

In this thesis work we aim to understand the link between polar localization and developmental function of the polarly localized transmembrane kinase, WALLFLOWER (WFL). In Chapter 2, we describe the mechanisms underlying establishment and maintenance of WFL polar localization at specific PM domains. In Chapter 3, we link WFL polar localization to its function in RH positioning in the longitudinal axis. Finally, in Chapter 4, we summarize this work and propose future experiments.

REFERENCES

Alassimone, J., Naseer, S., & Geldner, N. (2010). A developmental framework for endodermal differentiation and polarity. *Proceedings of the National Academy of Sciences of the United States of America*, *107*(11), 5214–5219.

Baster, P., & Friml, J. (2014). Auxin on the Road Navigated by Cellular PIN Polarity. In *Auxin and Its Role in Plant Development* (pp. 143–170). Springer Vienna.

Benfey, P. N., & Scheres, B. (2000). Root development. *Current Biology: CB*, *10*(22), R813–R815.

Breda, A. S., Hazak, O., & Hardtke, C. S. (2017). Phosphosite charge rather than shootward localization determines OCTOPUS activity in root protophloem. *Proceedings of the National Academy of Sciences of the United States of America*, *114*(28), E5721–E5730.

Campos, R., Goff, J., Rodriguez-Furlán, C., & Van Norman, J. M. (2020). The Arabidopsis Receptor Kinase IRK is Polarized and Represses Specific Cell Divisions in Roots. *Developmental Cell, 52*(2), 183–195.e4.

Costa, S., & Dolan, L. (2000). Development of the root pole and cell patterning in Arabidopsis roots. *Current Opinion in Genetics & Development*, *10*(4), 405–409.

Denninger, P., Reichelt, A., Schmidt, V. A. F., Mehlhorn, D. G., Asseck, L. Y., Stanley, C. E., Keinath, N. F., Evers, J.-F., Grefen, C., & Grossmann, G. (2019). Distinct RopGEFs Successively Drive Polarization and Outgrowth of Root Hairs. *Current Biology: CB*, *29*(11), 1854–1865.e5.

Dolan, L., Janmaat, K., Willemsen, V., Linstead, P., Poethig, S., Roberts, K., & Scheres, B. (1993). Cellular organisation of the Arabidopsis thaliana root. *Development* , *119*, 71–84.

Duan, Q., Kita, D., Li, C., Cheung, A. Y., & Wu, H.-M. (2010). FERONIA receptor-like kinase regulates RHO GTPase signaling of root hair development. *Proceedings of the National Academy of Sciences of the United States of America*, *107*(41), 17821–17826.

Gilroy, S., & Jones, D. L. (2000). Through form to function: root hair development and nutrient uptake. *Trends in Plant Science*, *5*(2), 56–60.

Grierson, C., Nielsen, E., Ketelaarc, T., & Schiefelbein, J. (2014). Root hairs. *The Arabidopsis Book / American Society of Plant Biologists*, *12*, e0172.

Habets, M. E. J., & Offringa, R. (2014). PIN-driven polar auxin transport in plant developmental plasticity: a key target for environmental and endogenous signals. *The New Phytologist*, *203*(2), 362–377.

Huang, G.-Q., Li, E., Ge, F.-R., Li, S., Wang, Q., Zhang, C.-Q., & Zhang, Y. (2013). Arabidopsis RopGEF4 and RopGEF10 are important for FERONIA-mediated developmental but not environmental regulation of root hair growth. *The New Phytologist*, *200*(4), 1089–1101.

Kwon, T., Sparks, J. A., Liao, F., & Blancaflor, E. B. (2018). ERULUS Is a Plasma Membrane-Localized Receptor-Like Kinase That Specifies Root Hair Growth by Maintaining Tip-Focused Cytoplasmic Calcium Oscillations. *The Plant Cell*, *30*(6), 1173–1177.

Łangowski, Ł., Wabnik, K., Li, H., Vanneste, S., Naramoto, S., Tanaka, H., & Friml, J. (2016). Cellular mechanisms for cargo delivery and polarity maintenance at different polar domains in plant cells. *Cell Discovery*, *2*, 16018.

Laskowski, M., Grieneisen, V. A., Hofhuis, H., Hove, C. A. T., Hogeweg, P., Marée, A. F. M., & Scheres, B. (2008). Root system architecture from coupling cell shape to auxin transport. *PLoS Biology*, *6*(12), e307.

Nakamura, M., & Grebe, M. (2018). Outer, inner and planar polarity in the Arabidopsis root. *Current Opinion in Plant Biology*, *41*, 46–53.

Naramoto, S. (2017). Polar transport in plants mediated by membrane transporters: focus on mechanisms of polar auxin transport. *Current Opinion in Plant Biology*, *40*, 8–14.

Petrásek, J., & Friml, J. (2009). Auxin transport routes in plant development. *Development* , *136*(16), 2675–2688.

Pfister, A., Barberon, M., Alassimone, J., Kalmbach, L., Lee, Y., Vermeer, J. E. M., Yamazaki, M., Li, G., Maurel, C., Takano, J., Kamiya, T., Salt, D. E., Roppolo, D., & Geldner, N. (2014). A receptor-like kinase mutant with absent endodermal diffusion barrier displays selective nutrient homeostasis defects. *eLife*, *3*, e03115.

Rodriguez-Furlán, C, Campos, R. C., Toth, J. N., & Van Norman, J. M. (2021). Distinct mechanisms underlie the contrasting polarity of IRK and KOIN, two LRR-RLKs involved in root tissue patterning [Manuscript submitted for publication].

Schiefelbein, J. W., & Somerville, C. (1990). Genetic Control of Root Hair Development in Arabidopsis thaliana. *The Plant Cell*, *2*(3), 235–243.

Schoenaers, S., Balcerowicz, D., Breen, G., Hill, K., Zdanio, M., Mouille, G., Holman, T. J., Oh, J., Wilson, M. H., Nikonorova, N., Vu, L. D., De Smet, I., Swarup, R., De Vos, W. H., Pintelon, I., Adriaensen, D., Grierson, C., Bennett, M. J., & Vissenberg, K. (2018). The Auxin-Regulated CrRLK1L Kinase ERULUS Controls Cell Wall Composition during Root Hair Tip Growth. *Current Biology: CB*, *28*(5), 722–732.e6.

Swarup, R., Friml, J., Marchant, A., Ljung, K., Sandberg, G., Palme, K., & Bennett, M. (2001). Localization of the auxin permease AUX1 suggests two functionally distinct hormone transport pathways operate in the Arabidopsis root apex. *Genes & Development*, *15*(20), 2648–2653.

Takano, J., Noguchi, K., Yasumori, M., Kobayashi, M., Gajdos, Z., Miwa, K., Hayashi, H., Yoneyama, T., & Fujiwara, T. (2002). Arabidopsis boron transporter for xylem loading. *Nature*, *420*(6913), 337–340.

Takano, J., Tanaka, M., Toyoda, A., Miwa, K., Kasai, K., Fuji, K., Onouchi, H., Naito, S., & Fujiwara, T. (2010). Polar localization and degradation of Arabidopsis boron transporters through distinct trafficking pathways. *Proceedings of the National Academy of Sciences of the United States of America*, *107*(11), 5220–5225.

Takano, J., Wada, M., Ludewig, U., Schaaf, G., von Wirén, N., & Fujiwara, T. (2006). The Arabidopsis major intrinsic protein NIP5;1 is essential for efficient boron uptake and plant development under boron limitation. *The Plant Cell*, *18*(6), 1498–1509.

Truernit, E., Bauby, H., Belcram, K., Barthélémy, J., & Palauqui, J.-C. (2012). OCTOPUS, a polarly localised membrane-associated protein, regulates phloem differentiation entry in Arabidopsis thaliana. *Development* , *139*(7), 1306–1315.

Van Norman, J. M. (2016). Asymmetry and cell polarity in root development. *Developmental Biology*, *419*(1), 165–174.

Wisniewska, J., Xu, J., Seifertová, D., Brewer, P. B., Ruzicka, K., Blilou, I., Rouquié, D., Benková, E., Scheres, B., & Friml, J. (2006). Polar PIN localization directs auxin flow in plants. *Science*, *312*(5775), 883.

Xun, Q., Wu, Y., Li, H., Chang, J., Ou, Y., He, K., Gou, X., Tax, F. E., & Li, J. (2020). Two receptor-like protein kinases, MUSTACHES and MUSTACHES-LIKE, regulate lateral root development in Arabidopsis thaliana. *The New Phytologist.* https://doi.org/10.1111/nph.16599

Zhu, S., Estévez, J. M., Liao, H., Zhu, Y., Yang, T., Li, C., Wang, Y., Li, L., Liu, X., Pacheco, J. M., Guo, H., & Yu, F. (2020). The RALF1-FERONIA Complex Phosphorylates eIF4E1 to Promote Protein Synthesis and Polar Root Hair Growth. *Molecular Plant, 13*(5), 698–716.

CHAPTER TWO: WALLFLOWER (WFL), a LRR-RLK, simultaneously localizes to opposite sides of epidermal hair cells in the *Arabidopsis* root

ABSTRACT

In the *Arabidopsis* root, polarized cells are frequently partitioned into distinct subdomains with unique features and functions. These subdomains can be defined by protein accumulation to a specific region at the plasma membrane, and are typically informed by a specific event or cue. We have identified WALLFLOWER (WFL), a leucine-rich repeat receptor-like kinase with asymmetric distribution at the inner face of the plasma membrane of epidermal cells. Specifically, in epidermal hair (H) cells within the elongation and differentiation zones, WFL exhibits a dual polar localization, accumulating at the inner polar domain as well as at the root hair initiation domain (RHID) and RH bulges. WFL asymmetric distribution and function is affected by deletion of the intracellular domains resulting in mislocalization to the outer polar domain of H cells and exclusion from RHIDs and bulges. Localization of full length WFL remains polar to the inner domain regardless of cell identity, however, removal of the intracellular domains results in varied localization patterns depending on cell type. Therefore, we propose that the intracellular domains of WFL are necessary to inform localization in individual cell types and developmental stages, and to direct its dual polarization in H cells.

INTRODUCTION

Cells are frequently partitioned into subdomains with unique features or functions and can therefore be described as polarized. Cell polarity can be defined as asymmetries in the localization of subcellular constituents and proteins and/or in cell morphology. Cell polarity can be achieved by preferential accumulation of proteins to specific plasma membrane (PM) domains, and is often followed by changes in morphological polarity. In plants, organisms whose cells are fixed in place due to the cell wall, polarized protein accumulation is required for diverse physiological and developmental processes, such as asymmetric cell division, localized cell growth, long- and short-range signal transduction, and directional transport (Breda et al., 2017; Petrásek & Friml, 2009; Takano et al., 2010). Furthermore, protein function, activity, and stability can be impacted by partitioning of the PM and therefore, cell polarity has tremendous regulatory potential in development (Łangowski et al., 2016; Nakamura & Grebe, 2018; Van Norman, 2016).

The *Arabidopsis* root is an excellent system to study various aspects of cell polarity and to link cell polarity to cellular or organ function and development. The root is composed of cells that are primarily cuboidal in shape with six discrete faces and organized into concentric layers around the central vascular tissues with individual files of cells extending through the longitudinal axis (Dolan et al., 1993, Figure 2.1A). In this axis, the root is divided into three developmental

zones: the meristematic, elongation, and differentiation zones, within which cells divide, elongate, or mature, respectively (Benfey & Scheres, 2000). These organizational features allow for straightforward analysis of protein localization, cell morphology, or developmental phenotypes in the root.

The root epidermis is composed of two cell types, hair (H) and nonhair cells (NH) and is an ideal system for studying protein accumulation to specific polar domains within the PM. Cells with H cell identity will form long, thin tubular extensions called root hairs (RHs), which are dramatic examples of morphological polarity in plant cells. RH development broadly occurs in 2 stages: initiation and tip growth via targeted secretion to the RH tip. The initiation of RHs requires the establishment of an additional polar domain within H cells, the root hair initiation domain (RHID). Establishment of the RHID requires polar localization of proteins to a confined region at the outer face and toward the rootward end of H cells. This leads to local formation of a bulge on the H cell surface that increases in size and becomes more defined (Grierson et al., 2014).

Polarized proteins are directed to specific PM domains through multiple endomembrane trafficking pathways. Polar localization of PIN-FORMED proteins (PINs) is well characterized and is facilitated by hyper-polar secretion of *de novo* protein coupled with recycling via endosomal compartments and restriction of lateral diffusion. Additionally, PIN1 polarity at the PM is disrupted by the

endocytic inhibitor Brefeldin A (BFA, Grebe et al., 2002). In contrast, polar localization of the LRR-RLKs, IRK and KOIN, is primarily directed by *de novo* secretion to the PM. Additionally, while IRK polar accumulation is directed via a BFA-sensitive mechanism, and KOIN is largely resistant, polar localization of both proteins is unaltered when treated with BFA. These observations indicate that the underlying mechanisms for polar localization of receptor-like kinases are not the same as those that have been described for PINs and emphasizes the complexity of polar localization for different proteins in plant cells.

Differential polar localization of proteins to specific PM membrane domains in different cell and tissue types implies that localization can be informed by cell and/or organ level cues. Consistent with this, localization of IRK changes depending on cell type and suggests that positional information is informed by adjacent cell types (Campos et al., 2020). In contrast, polar accumulation of KOIN remains the same regardless of cell type (Rodriguez-Furlán et al. 2021) suggesting that, similar to some nutrient transporters (Alassimone et al., 2010), its polar localization is directed by an organ level cue, originating from the inner cell layers of the root. Additionally, specific protein domains can direct polar localization of proteins at the PM. For example, KOIN localizes to the inner polar domain of endodermal cells and removal of its intracellular domains results in a nonpolar distribution. However, removal of IRK intracellular domains does not affect its polarity, indicating that the kinase domain does not direct polar

localization for all receptor-like kinases (Rodriguez-Furlán et al. 2021). Thus, the many factors that contribute to polar localization mechanisms of transmembrane proteins in plant cells remain largely unknown.

Here we identify a polarly localized LRR-RLK named WALLFLOWER (WFL) and describe the mechanisms of its polar localization in root cells. We show that WFL is localized to the inner polar domain in H cells and maintains this polarity as it accumulates at the RHID and bulges within the outer polar domain. This unusual localization positions WFL simultaneously on opposite sides of H cells. Our results also show that WFL polar accumulation and maintenance is mainly achieved by *de novo* protein synthesis and secretion through a BFA-dependent endomembrane trafficking pathway. We also demonstrate that WFL polarization is determined by its intracellular domains as expression of truncated WFL is mislocalized to the outer polar domain and, remarkably, fails to accumulate at RHIDs and bulges in H cells. Additionally, this truncated version of WFL appears to be directed to different cellular domains in different cell types indicating that the intracellular portion is needed for correct cell type-specific polar delivery. Thus, we propose that WFL is secreted via a BFA dependent pathway where polar delivery to distinct regions within the PM requires the WFL intracellular domains.

RESULTS

WFL is expressed primarily in LRC and epidermal cells

We identified WFL, encoded by At5g24100, as an LRR-RLK putatively involved in signaling and RH development based on its predominant expression in H cells in the elongation and differentiation zones (Brady et al., 2007; S. Li et al., 2016). To validate these data *in planta*, we drove expression of endoplasmic reticulum-localized green fluorescent protein (erGFP) with the putative *WFL* promoter (*pWFL*) in WT seedlings. *pWFL* activity was observed in the lateral root cap (LRC), but was not detectable in other cell types in the root meristem (Figure 2.1D-E). Consistent with the expression data, in elongation and differentiation zones, *pWFL* activity was detected in epidermal cells with preferential activity in H cells. Additionally, we detected *pWFL* activity in pericycle cells along with weaker activity in cortex cells (Figure 2.1B-C).

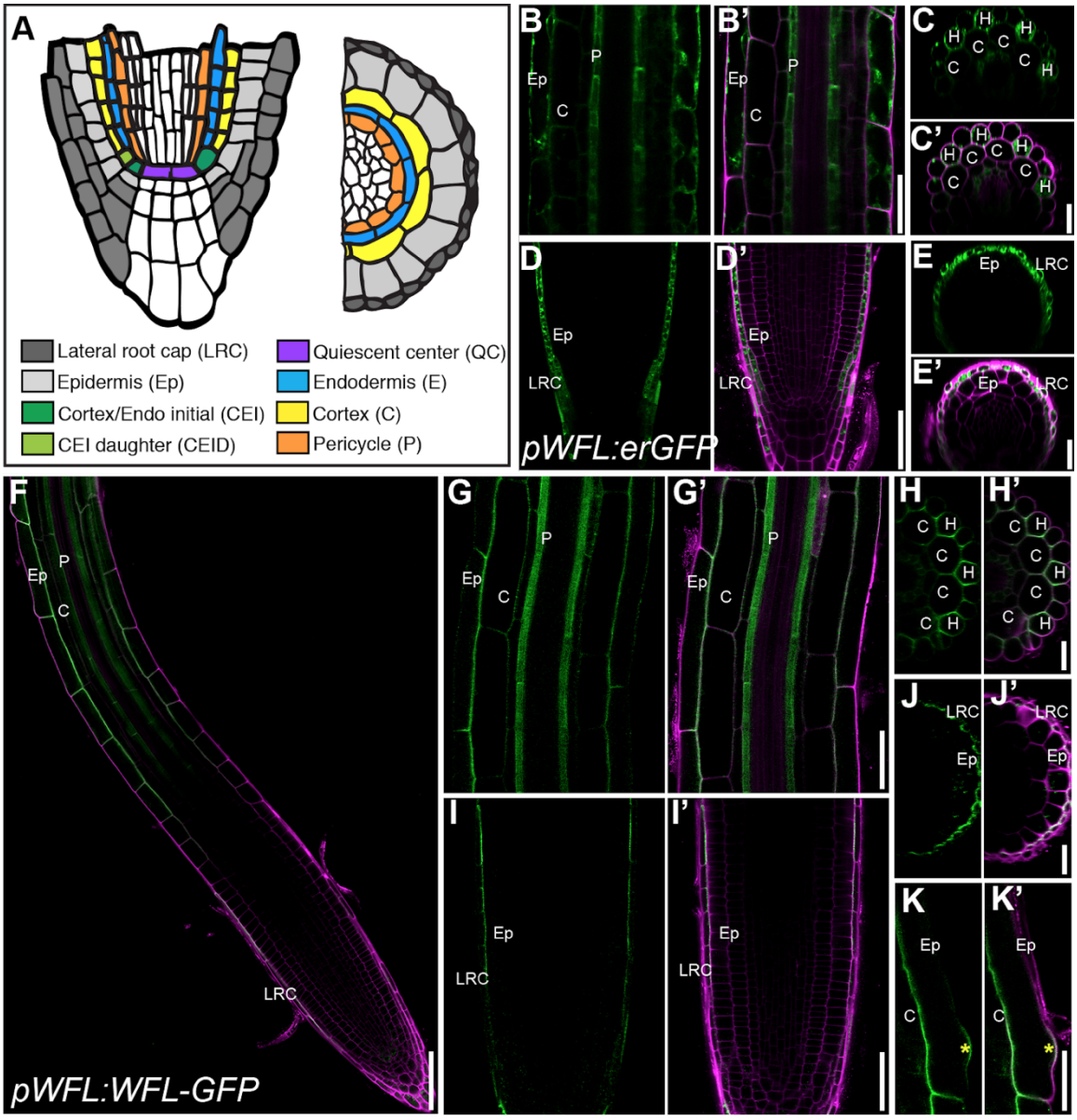
A
Lateral root cap (LRC)
Epidermis (Ep)
Cortex/Endo initial (CEI)
CEI daughter (CEID)
Quiescent center (QC)
Endodermis (E)
Cortex (C)
Pericycle (P)
B
B'
C
C'
D
D'
E
E'
Ep
LRC
C
P
H
pWFL:erGFP
F
G
G'
H
H'
I
I'
J
J'
K
K'
pWFL:WFL-GFP

Figure 2.1: *pWFL* is active in the lateral root cap and epidermis and WFL-GFP localizes to the inner polar domain of these cell types.
(A) Schematic representation of cell types in the Arabidopsis root in longitudinal and transverse views. (B-K) Confocal images of WT roots expressing (B-E) *pWFL:erGFP* and (F-K) *pWFL:WFL-GFP* and stained with propidium iodide (PI) to show cell outlines. Adjacent panels show GFP alone (**α**) and GFP + PI merged (**α**'), except in (F) where only the merged image is shown. (B and C) In the elongation and differentiation zones, *pWFL* is most active in pericycle and epidermal cells with higher activity (C) in H cells compared to NH cells. (D and E) In the meristematic zone, *pWFL* is active in the cell layers of the lateral root cap. (F) WFL-GFP localization in the root tip. (G and H) In the elongation and differentiation zones, WFL-GFP localizes to the inner polar domain of (G) epidermal cells with (H) preferential accumulation in H cells. (K) WFL-GFP also localizes to RH bulges (yellow asterisk). (I and J) WFL-GFP localizes to the inner polar domain of the outermost layer of the LRC. Abbreviations: LRC, lateral root cap; Ep, epidermis; C, cortex; P, pericycle; H, hair cell. Scale bars: 50 μm in (F); 25 μm in (B, D, G, and I); 10 μm in all others.

WFL-GFP accumulates asymmetrically at the PM

To examine WFL protein accumulation in *Arabidopsis* roots, we generated a WFL-GFP fusion under control of *pWFL* (*pWFL:WFL-GFP*). To examine WFL protein accumulation in Arabidopsis roots, we generated a WFL-GFP fusion under control of *pWFL* (*pWFL:WFL-GFP*). Interestingly, during our examination of *pWFL:WFL-GFP* in the WT (Col-0) background we observed that these roots appeared damaged more frequently than nontransgenic WT or *pWFL:erGFP* (in WT) roots, as evidenced by the presence of propidium iodide (PI) within cells. Incidents of cellular damage made roots difficult to image and were observed in >4 independent transgenic lines and by separate researchers (not shown). We hypothesized that these plants were sensitive to being mounted on slides, a type of mechanical stress, possibly due to a defect in cell wall integrity. To test this we transferred seedlings expressing *pWFL:WFL-GFP* from our standard growth medium to medium deficient in phosphate (-Pi), which has been reported to rigidify the walls of elongating root cells (Péret et al., 2011; Balzergue et al., 2017). After a 24-hour treatment on -Pi media, WFL-GFP localization was unaffected and these roots showed substantially less damage (PI penetration), which allowed us to image them more easily.

In the meristematic zone of WT roots expressing *pWFL:WFL-GFP*, we detect the protein only in the outermost cell layer of the LRC (Figure 2.1F, 2.1I-J). Consistent with the observed promoter activity, in the elongation and

differentiation zones WFL-GFP accumulates in cells of the epidermis, cortex, and pericycle (Figure 2.1F-H). In the LRC and epidermis, WFL-GFP is polarly localized to the inner polar domain of the PM (Figure 2.1F-J). Interestingly, in the epidermis WFL has higher accumulation in H cells and is also localized to the RH bulge (Figure 2.1F and K). In cortex cells we were unable to determine whether WFL-GFP was polarly localized due to the fluorescent signal from the adjacent epidermis. Also, in the pericycle, WFL-GFP signal appears diffuse, making it difficult to assess how WFL is distributed at the PM (Figure 2.1F and G). These results indicate that WFL is asymmetrically distributed along the PM in LRC and epidermal cells at different stages of differentiation.

WFL-GFP localizes to the inner polar domain regardless of cell type

With the endogenously expressed reporter, it was difficult to assess the polar distribution of WFL-GFP in the internal root cell layers. To address this, we misexpressed WFL-GFP using cell type- and tissue-specific promoters. WFL-GFP expressed under the control of the *WEREWOLF* promoter (*pWER,* M. M. Lee & Schiefelbein, 1999), which is specifically expressed in the epidermis and LRC (Figure 2.2A), was localized to the inner polar domain of these cell types (Figure 2.2B-C). We also examined WFL-GFP localization upon misexpression in the endodermis, cortex/endodermal initial (CEI), cortex/endodermal initial daughter (CEID), and quiescent center (QC, Figure 2.2D) using the *SCARECROW* promoter (*pSCR,* Levesque et al., 2006; Wysocka-Diller et al.,

2000) and found WFL-GFP localized to the inner polar domain of these cell types (Figure 2.2E-F); with the exception of the QC where WFL-GFP is oriented towards the stele (Figure 2E). Additionally, we misexpressed WFL-GFP in immature and mature cortex cells using the promoters of *CORTEX2* (*pCO2,* Heidstra et al., 2004; Paquette & Benfey, 2005) and *CORTEX* (*pC1,* Figure 2.2G J.-Y. Lee et al., 2006), respectively. We were unable to detect any GFP signal in immature cortex cells (not shown), but observed that WFL-GFP localized to the inner polar domain of mature cortex cells (Figure 2.2H-I). Altogether, our results show that polar localization of WFL-GFP is oriented inwards, towards the stele, in all cell types examined, suggesting that WFL localization to the inner polar domain is informed by a cue originating from the stele.

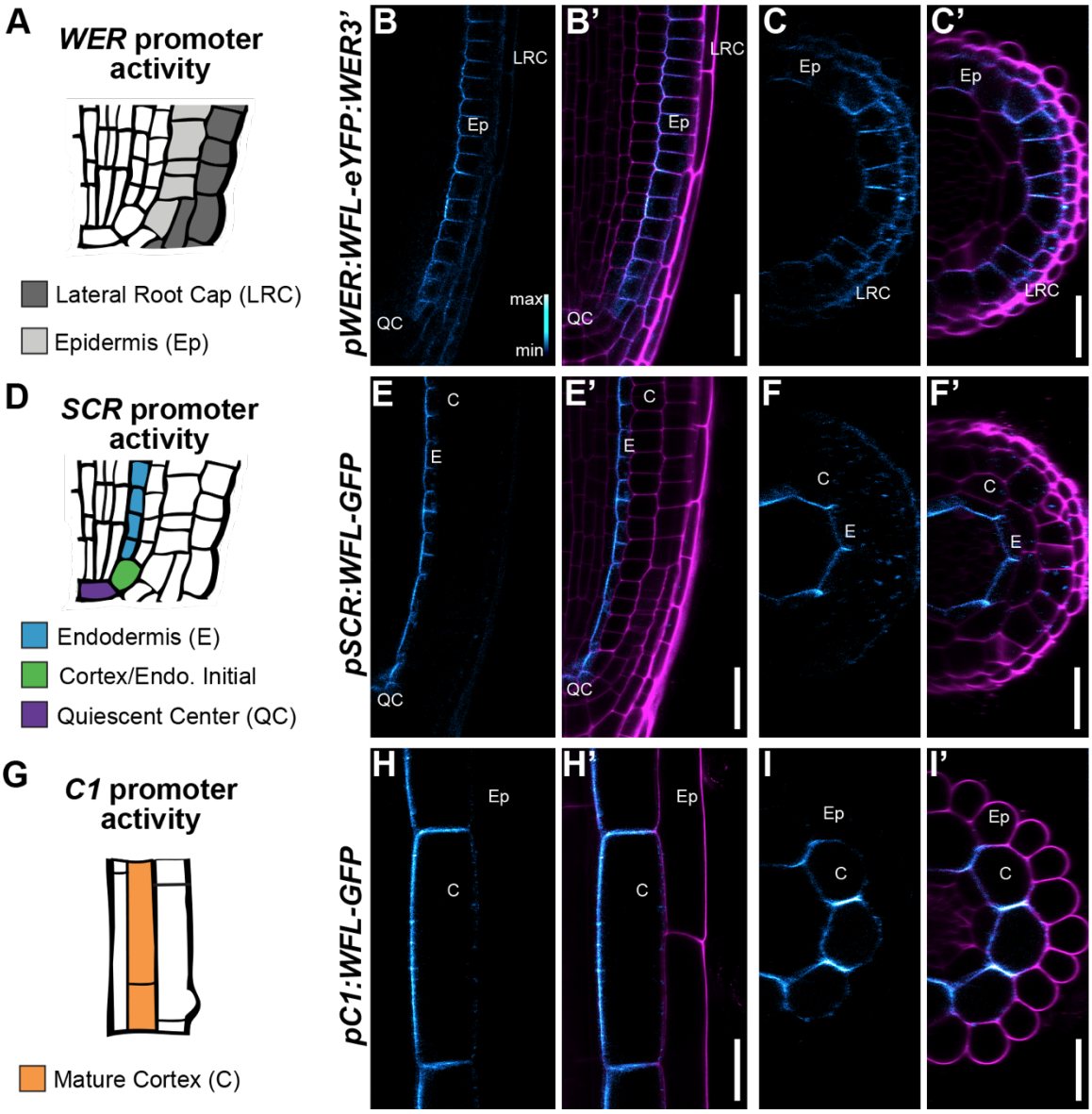
A
WER promoter activity
Lateral Root Cap (LRC)
Epidermis (Ep)
D
SCR promoter activity
Endodermis (E)
Cortex/Endo. Initial
Quiescent Center (QC)
G
C1 promoter activity
Mature Cortex (C)
pWER:WFL-eYFP:WER3'
pSCR:WFL-GFP
pC1:WFL-GFP
B
B'
C
C'
E
E'
F
F'
H
H'
I
I'
LRC
Ep
QC
max
min
C
E

Figure 2.2: WFL-GFP localizes to the inner polar domain regardless of cell type.
(A, D, and G) Schematics indicating activity of various promoters in specific cell layers. (A) *pWER* is active in LRC and epidermis. (D) *pSCR* is active in endodermis, CEI and QC. (G) *pC1* is active in mature cortex cells. (B, C, E, F, H, and I) Confocal images in longitudinal (B, E, and H) and transverse (C, F, I) planes of WT roots expressing WFL-GFP/YFP driven by cell layer-specific promoters (*pWER, pSCR,* and *pC1*) and stained with propidium iodide (PI) with adjacent panels showing GFP alone (false colored to show signal intensity, **α**) and GFP + PI merged (**α'**). (B-C) In the LRC and epidermis, WFL-eYFP localizes to the inner polar domain. (E-F) In endodermis and (H-I) the mature cortex, WFL-GFP localizes to the inner polar domain. Abbreviations: LRC, lateral root cap; Ep, epidermis; C, cortex; E, endodermis; QC, quiescent center. Scale bars: 25 μm.

WFL-GFP is dynamically trafficked to and from the PM

Proteins with polar localization can be directed to the PM by targeted secretion and/or maintained at the PM by endocytosis and recycling (Raggi et al., 2020; Rodriguez-Furlán et al., 2019). To understand how endomembrane trafficking contributes to the polar distribution of WFL-GFP at the PM, we performed a series of chemical treatments on roots expressing *pWFL* driven WFL-GFP (Figure 2.3A). Treatments with the endocytic inhibitor, BFA, generated intracellular accumulations consistent with BFA bodies (Figure 2.3B and F). These accumulations indicate that WFL-GFP is trafficked to the PM via a BFA-sensitive mechanism.

WFL-GFP accumulation into BFA bodies could be attributed solely to secretion of newly synthesized WFL-GFP or to protein returning to the PM after endocytosis and recycling to maintain the polarized pool of proteins. To investigate this, we first treated roots with cycloheximide (CHX), an inhibitor of protein synthesis and after 2 hours we observed a considerable reduction in WFL-GFP signal at the PM indicating a high rate of *de novo* protein secretion and turnover (Figure 2.3C and F). We next pre-treated the roots with CHX for 60 minutes and added BFA and incubated for an additional 60 minutes. After the co-treatment, WFL accumulation in BFA bodies was nearly abolished, with only a faint signal remaining detectable (Figure 2.3D and F). Therefore, the majority of the signal observed in BFA bodies can be attributed to the endomembrane trafficking of

newly synthesized WFL-GFP. Furthermore, after a 60-minute BFA treatment followed by wash out in the presence of CHX, WFL-GFP signal at the PM is recovered to values similar to the control (Figure 2.3E and F); again, indicating a high rate of protein turnover.

As our results indicate a high rate of protein turnover, we explored whether WFL is actively degraded by a Wortmannin (Wm)-sensitive pathway. Wm is an inhibitor of phosphoinositide synthesis that has been reported to inhibit endocytic trafficking of PM proteins towards the vacuole. Additionally, it has been shown that darkness induces internalization and trafficking of PM proteins to the vacuole and changes vacuolar pH, which delays degradation allowing fluorescent protein detection at the vacuole lumen (Kleine-Vehn et al., 2008). *pWFL:WFL-GFP* expressing roots were exposed to a 3 hour dark treatment to increase WFL-GFP transport to the vacuole evidenced by the GFP detection at the lumen in the epidermal cells (Figure 2.3G and G'). Upon a 2-hour treatment with Wm in dark conditions, we observed characteristic doughnut-shaped intracellular accumulations of WFL-GFP and a considerable decrease in fluorescent signal at the vacuole lumen (Figure 2.3H and 3H'). These results indicate that WFL-GFP is actively endocytosed and trafficked to the vacuole by a Wm sensitive pathway.

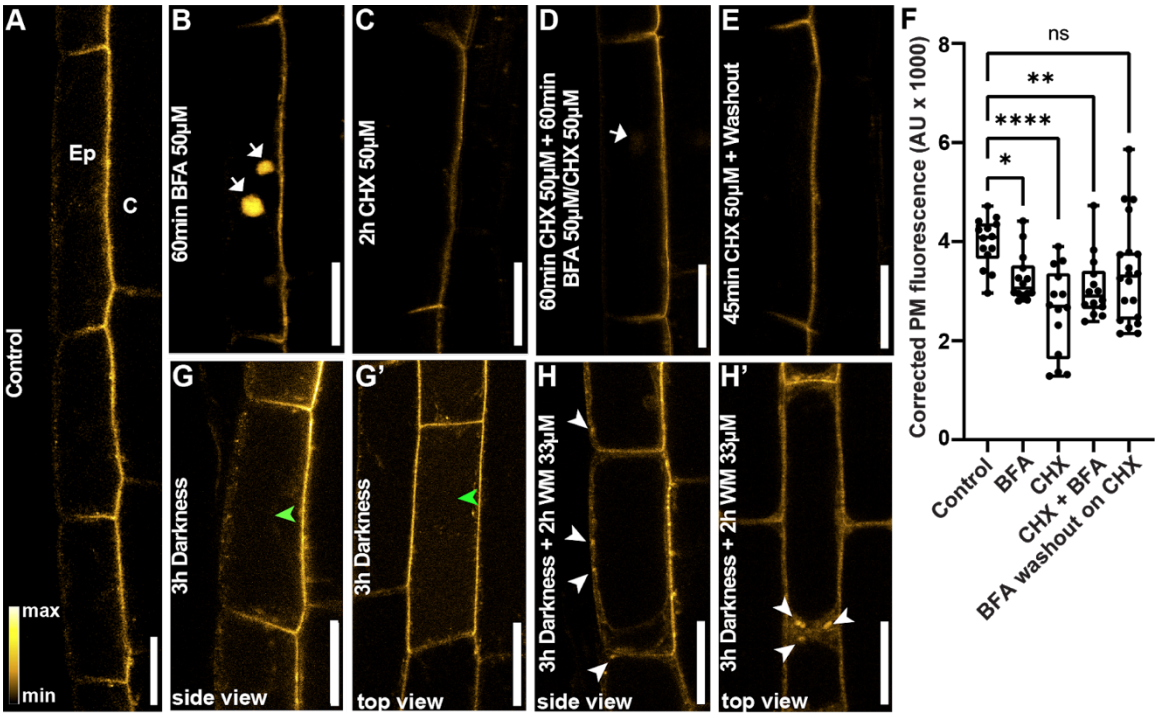

Figure 2.3: WFL-GFP is dynamically localized at the PM and trafficked to the vacuole for degradation. (A-F) Confocal images of unstained WT roots expressing *pWFL:WFL-GFP*. (A) In untreated control, WFL-GFP localizes to the inner polar domain of epidermal cells. (B) 60-minute BFA treatment results in WFL-GFP accumulation in BFA bodies. (C) 2-hour CHX treatment reduces WFL-GFP fluorescence at PM. (D) WFL-GFP weakly accumulates in BFA bodies upon cotreatment with CHX and BFA. White arrows indicate WFL-GFP in BFA bodies. (E) 2-hour CHX treatment followed by BFA washout does not result in appreciable signal recovery at the plasma membrane. (F) Graph shows the quantification of WFL corrected fluorescence intensity in arbitrary units (AU) at the PM after the indicated treatments. Data shown are representative results of experiments with at least three independent replicates. Bars indicate min. to max. values and 1-4 stars indicate statistical significance (P values ≤0.05, one-way ANOVA using Dunn's multiple comparison test). (G and G') 3-hour dark treatment induces WFL-GFP trafficking to vacuole. Green arrowheads indicate WFL-GFP accumulation in the vacuole lumen. (H and H') 2-hour Wortmannin (Wm) treatment results in accumulation of WFL-GFP in Wm bodies and inhibition of vacuolar trafficking. (G and H) Side view and (G' and H') top view of epidermal cells. White arrowheads indicate WFL-GFP in Wm bodies. Abbreviations: Ep, epidermis; C, cortex. Scale bars: 20 µm.

The WFL kinase domain is necessary for its polar distribution

To determine whether specific domains of WFL inform its polar accumulation at the PM, we created a truncated version by removing the intracellular region, which consists of the juxtamembrane (Jx) and kinase (K) domains, and fused this truncation to GFP under *pWFL* (*pWFL:WFL∆JxK-GFP*). Similar to full length WFL-GFP, we detected accumulation of WFL∆JxK-GFP in LRC cells of the meristematic zone, as well as in epidermal, cortex, and pericycle cells in the elongation and differentiation zones (Figure 2.4A-G). However, WFL localization to the inner polar domain and the RHID is strongly impacted. Indeed, WFL∆JxK-GFP polar localization appears to switch from the inner to the outer polar domain in LRC and epidermal cells (Figure 2.4A-G), and is specifically excluded from the RHID and bulge of H cells (Figure 2.4E-F). Similar results were obtained by removing only the kinase domain (*pWFL:WFL∆K-GFP*, Figure 2.5). Compared to WFL∆JxK-GFP, WFL∆K-GFP signal is lower, suggesting a reduction in secretion to the PM and/or protein instability.

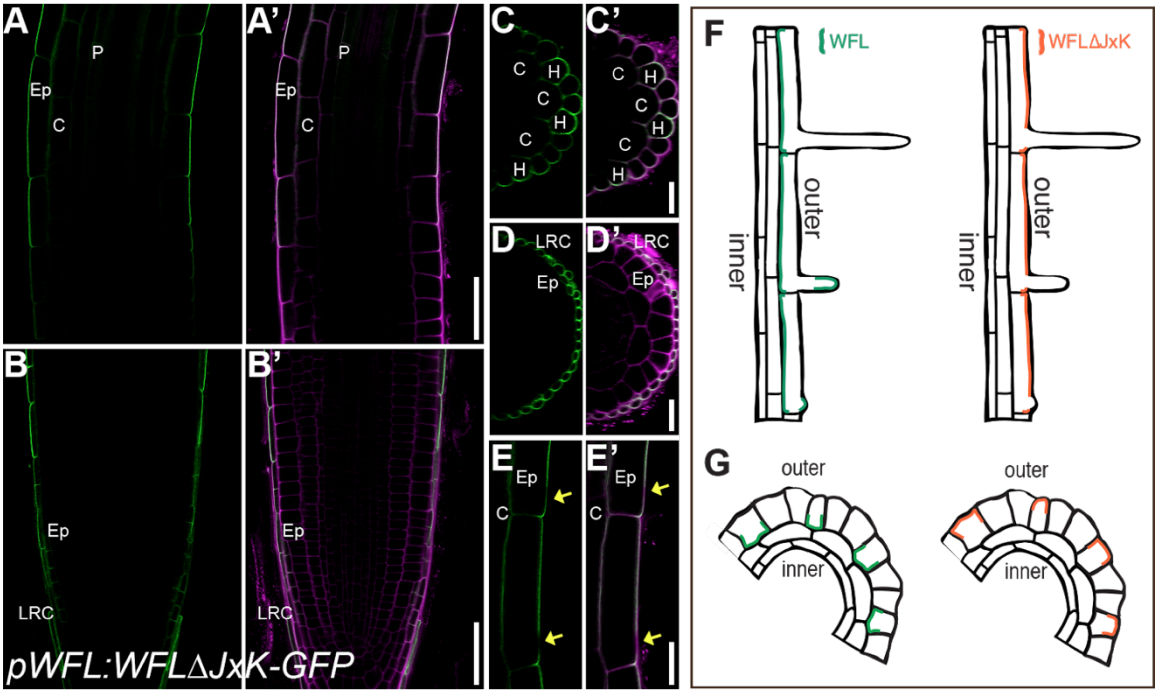

Figure 2.4: Deletion of the intracellular domains redirects WFL localization. (A-E) Confocal images of WT roots expressing WFLΔJxK-GFP driven by *pWFL* (*pWFL:WFLΔJxK-GFP)* and stained with propidium iodide (PI) to show cell outlines. Adjacent panels show GFP alone (**α**) and GFP + PI merged (**α**'). (A and C) In elongation and differentiation zones, WFLΔJxK-GFP localizes to the outer polar domain of epidermal cells with (C) preferential accumulation in H cells. (E) WFLΔJxK-GFP is excluded from RHIDs (yellow arrows). (B and D) WFLΔJxK-GFP localizes to the outer polar domain of the outermost cell layer of the LRC. (F and G) Schematics of WFL-GFP and WFLΔJxK-GFP localization in the (F) median longitudinal and (G) transverse views. Abbreviations: LRC, lateral root cap; Ep, epidermis; C, cortex; P, pericycle; H, hair cell. Scale bars: 25 μm in (A, B, and E); 10 μm in all others.

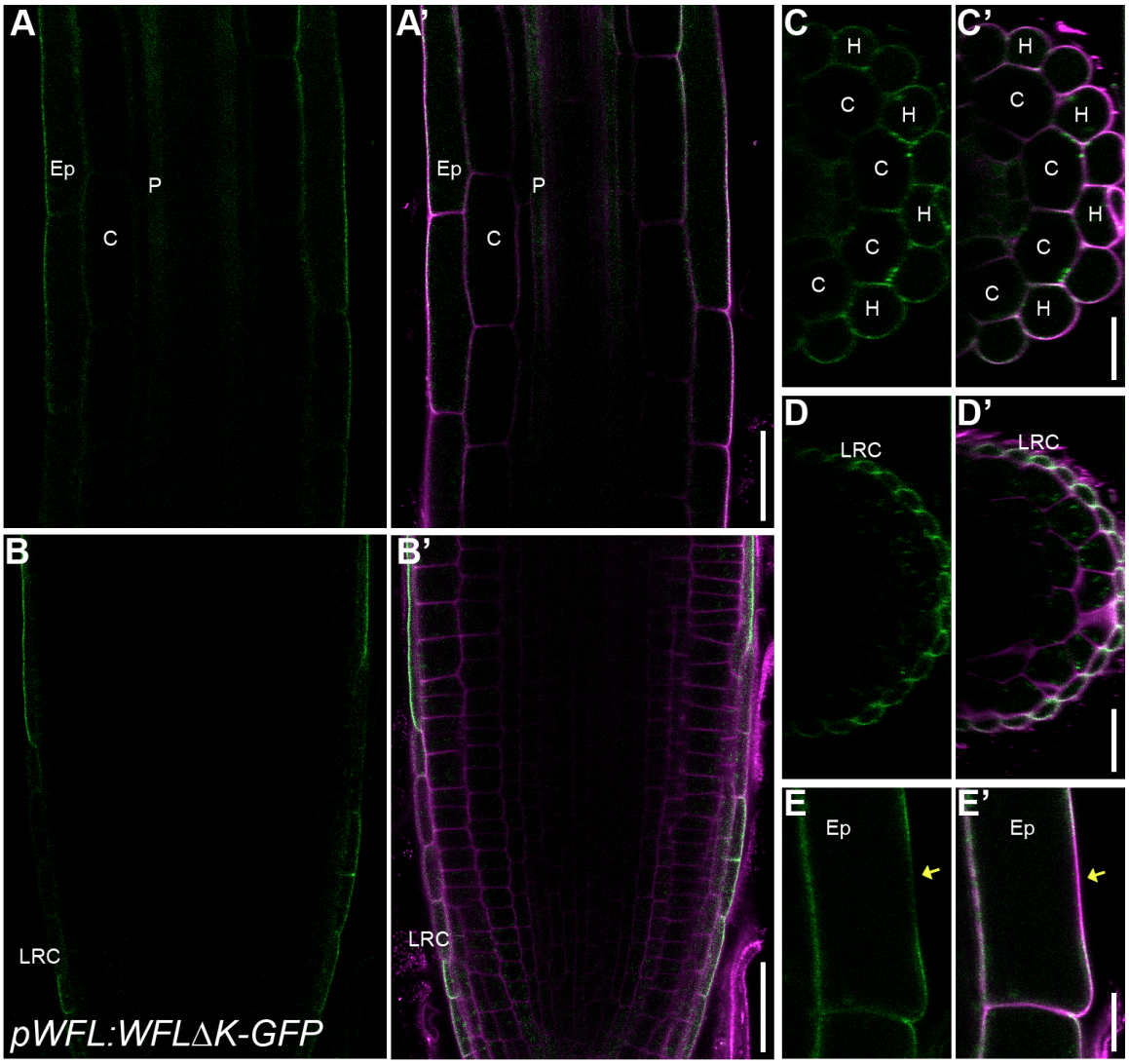

Figure 2.5: WFLΔK-GFP localizes to the outer polar domain of lateral root cap and epidermal cells.
(A-E) Confocal images of WT roots expressing WFLΔK-GFP driven by *pWFL* (*pWFL:WFL*ΔK-GFP) and stained with propidium iodide (PI) to show cell outlines. Adjacent panels show GFP alone (**α**) and GFP + PI merged (**α**'). (A and C) In elongation and differentiation zones, WFLΔK-GFP localizes to the outer polar domain of epidermal cells with (C) preferential accumulation in H cells. (E) WFLΔK-GFP is excluded from RHIDs. (B and D) WFLΔK-GFP localizes to the outer polar domain of the LRC. Abbreviations: LRC, lateral root cap; Ep, epidermis; C, cortex; H, hair cell. Scale bars: 25 μm in (A, B, and E); 10 μm in all others.

WFL intracellular domains are important for cell type-specific polar localization

WFL appears to be oriented by a stele-derived cue coordinating its inner polar distribution in every cell type. Therefore, we explored whether deleting the WFL cytoplasmic domain alters the ability of cells to localize WFL in response to this cue. When expressed from *pWER* and *pCO2,* WFL∆JxK-3xYFP preferentially localizes to the outer polar domain of LRC/epidermal and immature cortex cells near the QC, respectively (Figure 2.6A-B and 2.6E). Upon expression in mature cortex from *pC1,* WFL∆JxK-3xYFP was predominantly localized to the outer polar domain, however, some elongating cells showed nonpolar distribution of the protein (Figure 2.6C-D). Notably, when WFL∆JxK-3xYFP was expressed from *pSCR* we were unable to detect it in the primary root (not shown), however, in the endodermis and ground tissue stem cells of lateral roots, signal was detectable and showed a nonpolar distribution along the PM (Figure 2.6F). In contrast to full length WFL-GFP, there is no uniform interpretation of cues to polarize truncated WFL among the different cell types examined. These data indicate that WFL localization is highly regulated and its polarization towards the stele requires the intracellular domains, without which truncated WFL is misdirected in different cell types and developmental contexts.

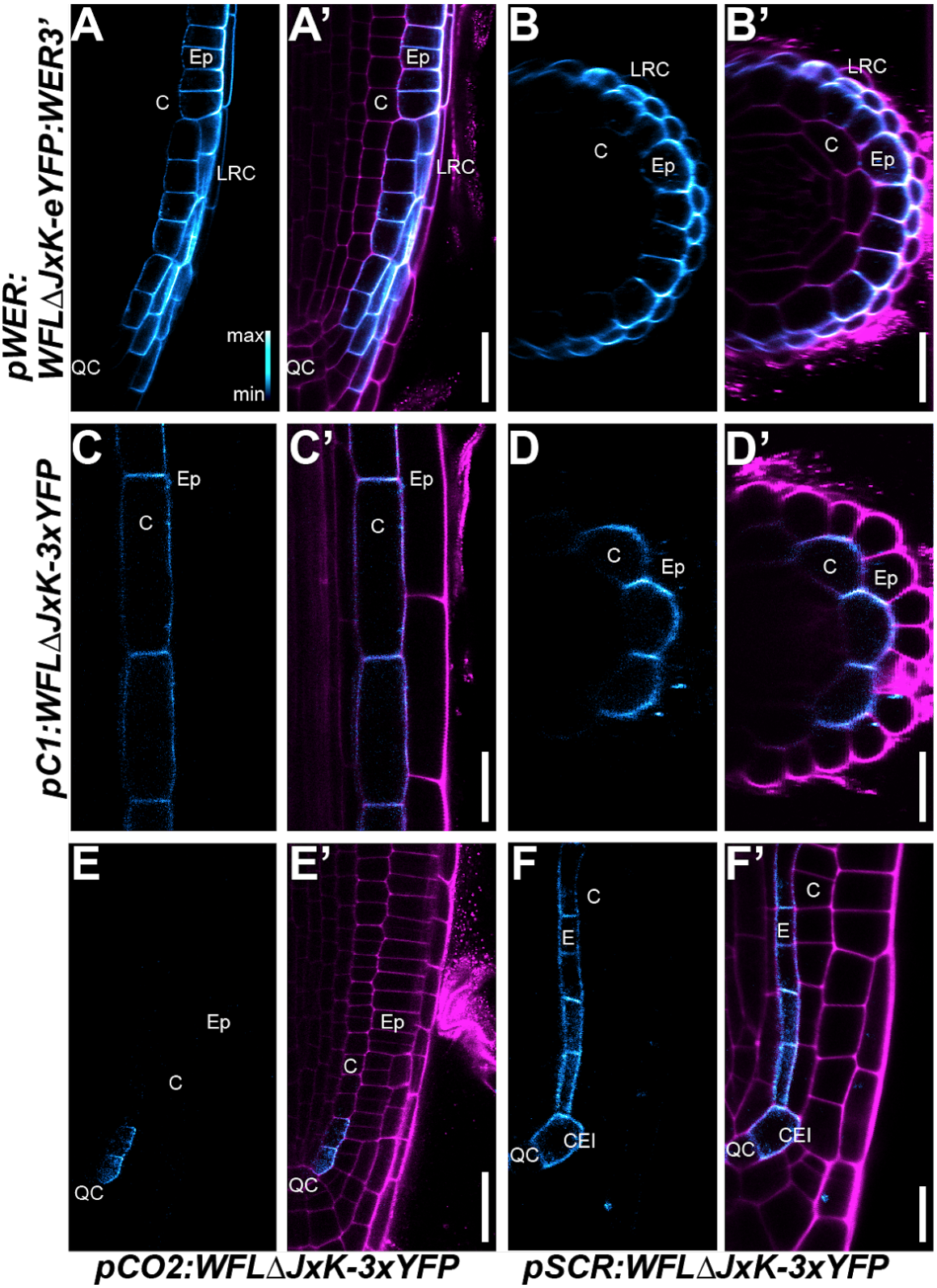
pWER:WFLΔJxK-eYFP:WER3'
pC1:WFLΔJxK-3xYFP
pCO2:WFLΔJxK-3xYFP
pSCR:WFLΔJxK-3xYFP
A
A'
B
B'
C
C'
D
D'
E
E'
F
F'
Ep
C
LRC
QC
max
min
E
CEI

Figure 2.6: Truncated WFL predominantly localizes to the outer polar domain or is nonpolar.
(A-F) Confocal images of WT roots expressing WFLΔJxK-eYFP/3xYFP driven by cell layer-specific promoters (*pWER, pCO2, pC1,* and *pSCR*) and stained with propidium iodide (PI) with adjacent panels showing YFP alone (false colored to show signal intensity, **α**) and YFP + PI merged (**α**'). (A, C, E, F) show images in longitudinal planes and (B and D) in the transverse planes. (A-B) In the LRC and epidermis, WFLΔJxK-eYFP localizes to the outer polar domain. (C-D) In mature cortex cells, WFLΔJxK-3xYFP preferentially localizes to the outer polar domain. (E) In immature cortex cells, WFLΔJxK-3xYFP localizes to the outer polar domain. (F) In ground tissue initials and endodermal cells of lateral roots, WFLΔJxK-3xYFP is nonpolar. Abbreviations: LRC, lateral root cap; Ep, epidermis; C, cortex; E, endodermis; CEI, cortex/endodermal initial; QC, quiescent center. Scale bars: 25 μm.

*WFL*Δ*JxK* is polarly distributed but actively excluded from WFL accumulation domains

To further characterize the opposite localization of WFL and WFLΔJxK in H cells, we closely followed their respective distributions during the different stages of RH development. WFL-GFP is present at the inner polar domain of elongating H cells and gradually appears at the RHID and is present at the bulge (Figure 2.7A). In contrast, WFLΔJxK-GFP is present at the outer polar domain in elongating H cells and gradually decreases its accumulation at RHIDs and is greatly reduced at the bulge (Figure 2.7B). Additionally, WFL-GFP shows the highest fluorescence intensity at the center of RHIDs and RH bulges (Figure 2.7C-F), whereas roots expressing *pWFL:WFL*Δ*JxK-GFP* exhibited lower fluorescence intensity at the center of RHIDs and RH bulges with higher fluorescence above and below the developing RH (Figure 2.7G-J). Together, these results indicate that WFL intracellular domains are important for polarized accumulation of WFL at specific domains of the PM.

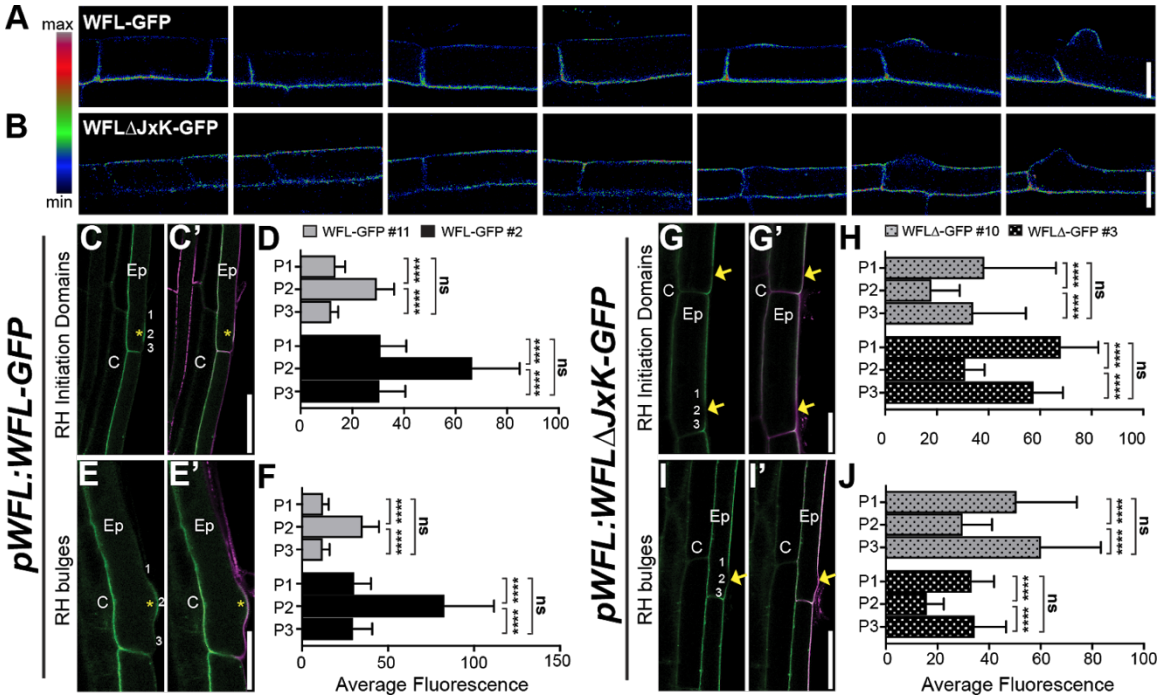

Figure 2.7: WFL-GFP and WFLΔJxK-GFP have inverse localization patterns at RHIDs and bulges.

(A and B) Confocal images of WT roots expressing *pWFL* driven (A) WFL-GFP and (B) WFLΔJxK-GFP (GFP false colored to show signal intensity). As H cell development progresses, (A) WFL-GFP localizes to RHIDs and bulges while (B) WFLΔJxK-GFP is excluded from these sites. (C, E, G, and I) Confocal images of WT roots expressing *pWFL* driven (C and E) WFL-GFP and (G and I) WFLΔJxK-GFP and stained with propidium iodide (PI) with adjacent panels showing GFP alone (**α**) and GFP + PI merged (**α'**). (C and E) WFL-GFP localizes to the inner polar domain of H cells and to (C) RHIDs as well as (C) bulges in the outer polar domain. (D and F) Quantification of fluorescence intensity at 3 positions - above, at the center, and below (D) RHIDs and (F) bulges in two independent transgenic lines. (G and I) WFLΔJxK-GFP localizes to the outer polar domain of epidermal cells and is excluded from (G) RHIDs and (I) bulges. (H and J) Quantification of fluorescence intensity above, below, and at (H) RHIDs and (I) bulges in two independent transgenic lines. For graphs: error bars, SD; student's t test, **** $p<0.0001$. Two different transgenic lines for each reporter were used as biological replicates, with n= 15-20 roots and 2-3 cells per root per replicate. Yellow asterisks and arrows indicate sites of RH initiation and bulges for WFL-GFP and WFLΔJxK-GFP, respectively. Numbers indicate positions of fluorescence intensity measurements relative to RH apex, 1= above, 2= center, 3= below. Abbreviations: Ep, epidermis; C, cortex. Scale bars: 20 μm in (A and B) 50 μm in (C and I); 25 μm in (E and G).

DISCUSSION

We were intrigued by the distinctive polar localization of WFL and sought to understand the mechanisms that govern its polarity. Endomembrane protein trafficking is closely related to the establishment and maintenance of PM protein polarity (Muroyama & Bergmann, 2019; Raggi et al., 2020; Rodriguez-Furlán et al., 2019) Our results indicate that WFL polarity at the PM is primarily maintained by constant cycles of secretion and degradation. The biosynthetic secretory traffic is directed through a BFA sensitive pathway. However, BFA interference of protein delivery does not alter polarity as has been described for PIN1 proteins (Tanaka et al., 2014). Additionally, endocytosis and recycling does not appear to be needed to maintain the pool of WFL protein at the PM, instead relying solely on *de novo* protein synthesis.

Upon removal of the intracellular domains, WFL∆JxK-GFP is secreted into H cell domains where there is normally no full length WFL accumulation. Furthermore, WFL∆JxK-GFP appears to be excluded from the inner polar domain and from the RHID. The inverse distribution of these two proteins is particularly striking and suggests that their secretion to the PM is subject to strict regulation. It is unclear how this contrasting localization is achieved, but it could be explained by interaction or lack of interaction with other proteins. Recently, polar localization of GUANINE NUCLEOTIDE EXCHANGE FACTOR3 (GEF3) to the RHID was shown to be necessary for RHO-RELATED PROTEIN FROM PLANTS 2 (ROP2)

recruitment to this site (Denninger et al., 2019). Therefore, it is possible that in the absence of its intracellular domains, WFLΔJxK-GFP is unable to interact with a binding partner that is also polarized at the RHID. Interaction through the WFL cytoplasmic domain with a protein also specifically localized at the RHID and excluded from the rest of the outer polar domain could explain its polar localization. Further research will be necessary to identify such partners.

The mislocalization of WFLΔJxK-GFP to the outer polar domain stresses the importance of the kinase domain for its normal localization. Similar to WFL, removal of the intracellular domains of the LRR-RLK, KOIN, results in nonpolar localization in root endodermal cells. In contrast, removal of the intracellular domains of another LRR-RLK, IRK, does not affect its polar localization (Rodriguez-Furlán et al. 2021). The different localization outcomes for these three truncated versions of polarized LRR-RLKs indicates that polarity of plant transmembrane receptors is not solely dependent upon the kinase domain.

Localization of full length WFL appears to be informed by a cue that originates from the stele. WFL-GFP localization is similar to laterally polar transport proteins in that nutrient transporters, such as BOR1 and NIP5;1, also localize to the same lateral polar domain, regardless of cell type (Alassimone et al., 2010). In contrast, polar localization of IRK is informed locally by adjacent cells and changes depending on cell type (Campos et al., 2020). These observations suggest that

cells interpret and respond to positional information to localize LRR-RLKs in multiple ways.

While polar localization of full length WFL is likely informed by organ-level polarity cues, removal of the intracellular domains indicates that the kinase domain is essential for cells to interpret these cues and localize WFL. Unlike WFL-GFP, misexpression of WFL∆JxK-GFP reveals differential localization depending on cell identity and developmental context. WFL∆JxK-GFP localizes to the outer polar domain of epidermal cells and immature cortex cells, whereas in mature cortex cells, WFL∆JxK-GFP preferentially accumulates at the outer polar domain, but is less polarized. Strikingly, WFL∆JxK-GFP is absent from endodermal cells of the primary root but, in lateral roots, exhibits nonpolar localization in the endodermis. Therefore, it is possible that lack of the intracellular domain re-directs the protein to different secretion pathways in different cell types. This hypothesis is consistent with the existence of multiple endomembrane trafficking pathways governing polar localization of transmembrane receptors in plants (R. Li et al., 2017). These results emphasize the necessity of the intracellular domains to direct WFL localization, which is informed by context-specific factors that take into account cell type and developmental stage.

Our observations demonstrate that WFL is a polarly localized LRR-RLK with dual polar localization to the inner and outer polar domains of root epidermal H cells. The importance of the WFL intracellular domains is highlighted by the change in WFL localization from the inner to the outer polar domain of epidermal H cells. This is further underscored by the exclusion of WFL∆JxK-GFP from RHIDs and bulges. To the best of our knowledge, WFL is the first transmembrane receptor that has been identified with this type of opposite localization pattern. While the function of WFL remains unknown, the specific polar localization of WFL-GFP to RHIDs and bulges coupled with root sensitivity to mechanical force, makes it tempting to speculate that WFL may have a role in RH development.

MATERIALS AND METHODS

Plant materials and growth conditions

The *Arabidopsis thaliana* Columbia-0 accession was used as the wild type. Standard growth media consisted of 0.5x, 1x, or 1x -Pi Murashige and Skoog salts (Caisson labs), 0.5 g/L MES (EMD), 1% sucrose, pH 5.7, and 1% agar (Difco), unless otherwise noted. Seeds were surface sterilized with chlorine gas, stratified in tubes at 4°C for 2-3 days and then plated on 100 millimeter plates with standard growth medium. Plates were then placed vertically in a Percival incubator under long day conditions (16 h light/8 h dark) at a constant temperature of 22°C. Plates were sealed with parafilm for experimental analyses.

Seedlings were typically examined between 4-7 days post-stratification (dps). Details for individual experiments are listed in figure legends and/or below.

Vector Construction and Plant Transformation

Transcriptional and translational reporter genes were constructed by standard molecular biology methods and utilizing Invitrogen Multisite Gateway® technology (Carlsbad, USA). A region 4.1 kb upstream of the *WFL* (At5g24100) start codon was amplified from Col-0 genomic DNA and recombined into the Invitrogen pENTR™ 5'-TOPO® TA vector. For the transcriptional reporter, the promoter drove endoplasmic reticulum-localized green fluorescent protein (erGFP) as previously described (Van Norman et al., 2014). For translational fusions, the genomic fragment encoding *WFL* from the ATG up to, but excluding the stop codon (including introns, 2.0 kb), was amplified from Col-0 genomic DNA and recombined into the Invitrogen pENTR™ DIRECTIONAL TOPO® (pENTR-D-TOPO) vector and fused to a C-terminal GFP tag as previously described (Van Norman et al., 2014). Specific primers for *WFL* cloning are listed in Table 2.1.

WFL-GFP and WFLΔJxK-GFP were driven by cell type-specific promoters (*pSCR*$_{2.0}$*, pCO*$_2$*, pC1, pUBQ10,* and *pWER)* as previously described (Campos et al., 2020; J.-Y. Lee et al., 2006). Due to the relatively low fluorescent signal of *pWFL:WFLΔJxK-GFP,* WFLΔJxK-GFP misexpression reporters for these

truncations were fused to 3xYFP. *pC1* was received in (Gateway Compatible) pENTR™ P4P1R TA vector from the lab of Philip Benfey, Duke University (Durham, NC, USA). The epidermal translational reporter *pWER:WFL-eYFP:WER3'* was generated as previously described (Campos et al., 2020). The various Gateway compatible fragments were recombined together with the dpGreen-BarT (J.-Y. Lee et al., 2006) or dpGreen-NorfT destination vector. The dpGreenNorfT was generated by combining the backbone of dpGreenBarT with the p35S::tpCRT1 and terminator insert from pGII0125. Within the target region of the dpGreenBarT, one AclI site was mutated with the QuickChangeXL kit (Stratagene). Plasmids were amplified in ccdB-resistant E.coli and plasmids prepped with a Bio Basic Plasmid DNA Miniprep kit. 34uL of the modified dpGreenBarT and unmodified pGII0125 were digested with 1ul each FspI and AclI in CutSmart buffer (NEB) for 1hr at 37C. Digests were subjected to gel electrophoresis on a 1% agarose gel. The 5866 bp fragment from the dpGreenBarT and 2592 bp fragment from the pGIIII0125 were extracted with a Qiagen MinElute Gel Extraction kit. The fragments were then ligated at 1:1 volumetric ratio (20ng vector; 8.8ng insert) using T4 DNA ligase incubated at 16C overnight before transformation into ccdB-resistant E.coli.

Expression constructs were then transformed into Col-0 plants by the floral dip method (Clough & Bent, 1998) using Agrobacterium strain GV3101 (Koncz et al., 1992) and transformants were identified using standard methods. For each

reporter gene, T2 lines with a 3:1 ratio of resistant to sensitive seedlings, indicating the transgene is inherited as a single locus, were selected for propagation. These T2 plants were allowed to self and among the subsequent T3 progeny, those with 100% resistant seedlings, indicating that the transgene was homozygous, were used in further analyses. For each reporter, at least three independent lines with the same relative expression levels and localization pattern were selected for imaging by confocal microscopy.

Confocal Microscopy and Image Analysis

Roots were stained with ~10 μM propidium iodide (PI) solubilized in water for 1-2 min. Imaging was performed via laser scanning confocal microscopy on a Leica SP8 upright microscope equipped with a water-corrected 40x objective and housed in the Van Norman lab. Root meristems were visualized in the median longitudinal or transverse planes. Images were generated using PMT and HYD detectors with the pinholes adjusted to 1 airy unit for each wavelength and system settings were as follows: GFP (excitation 488 nm, emission 492-530 nm), YFP (excitation 514 nm, emission 515-550 nm) and PI (excitation 536 nm, emission 585-660 nm). Unless otherwise indicated, all confocal images are either median longitudinal of roots or transverse sections acquired in the meristematic, elongation, and/or differentiation zones. All plants used for reporter expression imaging were grown on 1x MS with the exception of the roots expressing *pWFL:WFL-GFP* in Figure 2.1 and Figure 2.7C and 2.7E which were grown on 1x MS for 6 days and then

transferred to 1x MS -Pi plates for 24 hours. Localization of WFL-GFP was unaffected by -Pi treatment.

For GFP fluorescence intensity measurements of *pWFL:WFL-GFP* and *pWFL:WFL∆JxK-GFP*, seedlings were grown side-by-side on 0.5x MS plates until 5 dps. RHIDs and RH bulges were selected for analysis at the beginning of the differentiation zone. GFP intensity was measured using Leica (LAS X) quantification software at 3 different positions across the outer epidermal edge. The positions were assigned as follows: Position 1, the area just above the RHID or RH bulge; Position 2, at center of the RHID or RH bulge; Position 3, the area just below the RHID or RH bulge. The maximum GFP intensity was recorded for all 3 positions in 2 biological replicates for 15-20 roots per replicate and GFP intensity was measured in 2-3 cells per root. Representative images of RH initiation sites and RH bulges were chosen for each genotype for the figure.

Chemical Treatments

Treatments with small molecules were performed using *pWFL:WFL-GFP* in the Col-0 background seedlings grown on 0.5x MS plates grown until 5 dps. Seedlings were then incubated in liquid 0.5x MS containing one or a combination of the following chemicals: Brefeldin A (BFA) (Sigma-Aldrich) was dissolved in dimethyl sulfoxide (DMSO) (Calbiochem, Cat #317275) in 50 mM stocks and added to the media at a final concentration of 50 µM for 1 hour or other indicated

times. Cycloheximide (CHX) (Sigma-Aldrich, Cat #C7698) was added from a 50 mM aqueous stock to a final concentration of 50 uM for 2 hours or other indicated time. Wortmannin (Wm) (Sigma-Aldrich) was dissolved in DMSO and used at 33 uM for 2 hours. In control (mock) experiments, seedlings were incubated in the same media containing an equal amount (0.05% to 0.1%) DMSO.

Quantification and Statistical Analysis

The Leica LAS X software, as well as ImageJ were used for post-acquisition confocal image processing. Graphs were generated using PRISM8 (GraphPad Software, https://www.graphpad.com/, San Diego, USA). Microsoft Excel was used for student's t tests. The exact value of n, what n represents, the number of biological or technical replicates is indicated in each of the relevant figure legends and tables.

Primer Name	Sequence (5'->3')
WFLcod_F	caccATGAGTAGAGGAAGATCTTTCATCTTC
WFLcod_R	GTCTCTCTCAATCTCTTCCAAAGTC
WFLpro_F	CGAAGAGTCATGTTGGTCATGTT
WFLpro_R	CTTCTTACTAATTGTTATGTGATGGA
WFLcod_truncR	TGTCTCTGACTTCCTCTGCCT
WFLcod_trunc-K_R	TGCAGAAGCTATCAACAAGTCTTC

Table 2.1. Cloning primers related to Figures 2.1-2.7.

REFERENCES

Alassimone, J., Naseer, S., & Geldner, N. (2010). A developmental framework for endodermal differentiation and polarity. *Proceedings of the National Academy of Sciences of the United States of America*, *107*(11), 5214–5219.

Balzergue, C., Dartevelle, T., Godon, C., Laugier, E., Meisrimler, C., Teulon, J.-M., Creff, A., Bissler, M., Brouchoud, C., Hagège, A., Müller, J., Chiarenza, S., Javot, H., Becuwe-Linka, N., David, P., Péret, B., Delannoy, E., Thibaud, M.-C., Armengaud, J., … Desnos, T. (2017). Low phosphate activates STOP1-ALMT1 to rapidly inhibit root cell elongation. *Nature Communications*, *8*, 15300.

Benfey, P. N., & Scheres, B. (2000). Root development. *Current Biology: CB*, *10*(22), R813–R815.

Brady, S. M., Orlando, D. A., Lee, J.-Y., Wang, J. Y., Koch, J., Dinneny, J. R., Mace, D., Ohler, U., & Benfey, P. N. (2007). A high-resolution root spatiotemporal map reveals dominant expression patterns. *Science*, *318*(5851), 801–806.

Breda, A. S., Hazak, O., & Hardtke, C. S. (2017). Phosphosite charge rather than shootward localization determines OCTOPUS activity in root protophloem. *Proceedings of the National Academy of Sciences of the United States of America*, *114*(28), E5721–E5730.

Campos, R., Goff, J., Rodriguez-Furlán, C., & Van Norman, J. M. (2020). The Arabidopsis Receptor Kinase IRK is Polarized and Represses Specific Cell Divisions in Roots. *Developmental Cell, 52*(2), 183–195.e4.

Clough, S. J., & Bent, A. F. (1998). Floral dip: a simplified method for Agrobacterium-mediated transformation of Arabidopsis thaliana. *The Plant Journal: For Cell and Molecular Biology*, *16*(6), 735–743.

Denninger, P., Reichelt, A., Schmidt, V. A. F., Mehlhorn, D. G., Asseck, L. Y., Stanley, C. E., Keinath, N. F., Evers, J.-F., Grefen, C., & Grossmann, G. (2019). Distinct RopGEFs Successively Drive Polarization and Outgrowth of Root Hairs. *Current Biology: CB*, *29*(11), 1854–1865.e5.

Dolan, L., Janmaat, K., Willemsen, V., Linstead, P., Poethig, S., Roberts, K., & Scheres, B. (1993). Cellular organisation of the Arabidopsis thaliana root. *Development* , *119*, 71–84.

Grebe, M., Friml, J., Swarup, R., Ljung, K., Sandberg, G., Terlou, M., Palme, K., Bennett, M. J., & Scheres, B. (2002). Cell polarity signaling in Arabidopsis involves a BFA-sensitive auxin influx pathway. *Current Biology: CB*, *12*(4), 329–334.

Grierson, C., Nielsen, E., Ketelaarc, T., & Schiefelbein, J. (2014). Root hairs. *The Arabidopsis Book / American Society of Plant Biologists*, *12*, e0172.

Heidstra, R., Welch, D., & Scheres, B. (2004). Mosaic analyses using marked activation and deletion clones dissect Arabidopsis SCARECROW action in asymmetric cell division. *Genes & Development*, *18*(16), 1964–1969.

Kleine-Vehn, J., Dhonukshe, P., Swarup, R., Bennett, M., & Friml, J. (2006). Subcellular trafficking of the Arabidopsis auxin influx carrier AUX1 uses a novel pathway distinct from PIN1. *The Plant Cell*, *18*(11), 3171–3181.

Kleine-Vehn, J., Leitner, J., Zwiewka, M., Sauer, M., Abas, L., Luschnig, C., & Friml, J. (2008). Differential degradation of PIN2 auxin efflux carrier by retromer-dependent vacuolar targeting. *Proceedings of the National Academy of Sciences of the United States of America*, *105*(46), 17812–17817.

Koncz, C., Németh, K., Rédei, G. P., & Schell, J. (1992). T-DNA insertional mutagenesis in Arabidopsis. *Plant Molecular Biology*, *20*(5), 963–976.

Łangowski, Ł., Wabnik, K., Li, H., Vanneste, S., Naramoto, S., Tanaka, H., & Friml, J. (2016). Cellular mechanisms for cargo delivery and polarity maintenance at different polar domains in plant cells. *Cell Discovery*, *2*, 16018.

Lee, J.-Y., Colinas, J., Wang, J. Y., Mace, D., Ohler, U., & Benfey, P. N. (2006). Transcriptional and posttranscriptional regulation of transcription factor expression in Arabidopsis roots. *Proceedings of the National Academy of Sciences of the United States of America*, *103*(15), 6055–6060.

Lee, M. M., & Schiefelbein, J. (1999). WEREWOLF, a MYB-related protein in Arabidopsis, is a position-dependent regulator of epidermal cell patterning. *Cell*, *99*(5), 473–483.

Levesque, M. P., Vernoux, T., Busch, W., Cui, H., Wang, J. Y., Blilou, I., Hassan, H., Nakajima, K., Matsumoto, N., Lohmann, J. U., Scheres, B., & Benfey, P. N. (2006). Whole-genome analysis of the SHORT-ROOT developmental pathway in Arabidopsis. *PLoS Biology*, *4*(5), e143.

Li, R., Rodriguez-Furlán, C., Wang, J., van de Ven, W., Gao, T., Raikhel, N. V., & Hicks, G. R. (2017). Different Endomembrane Trafficking Pathways Establish Apical and Basal Polarities. *The Plant Cell*, *29*(1), 90–108.

Li, S., Yamada, M., Han, X., Ohler, U., & Benfey, P. N. (2016). High-Resolution Expression Map of the Arabidopsis Root Reveals Alternative Splicing and lincRNA Regulation. *Developmental Cell*, *39*(4), 508–522.

Muroyama, A., & Bergmann, D. (2019). Plant Cell Polarity: Creating Diversity from Inside the Box. *Annual Review of Cell and Developmental Biology*, *35*, 309–336.

Nakamura, M., & Grebe, M. (2018). Outer, inner and planar polarity in the Arabidopsis root. *Current Opinion in Plant Biology*, *41*, 46–53.

Paquette, A. J., & Benfey, P. N. (2005). Maturation of the ground tissue of the root is regulated by gibberellin and SCARECROW and requires SHORT-ROOT. *Plant Physiology*, *138*(2), 636–640.

Péret, B., Clément, M., Nussaume, L., & Desnos, T. (2011). Root developmental adaptation to phosphate starvation: better safe than sorry. *Trends in Plant Science*, *16*(8), 442–450.

Petrásek, J., & Friml, J. (2009). Auxin transport routes in plant development. *Development* , *136*(16), 2675–2688.

Raggi, S., Demes, E., Liu, S., Verger, S., & Robert, S. (2020). Polar expedition: mechanisms for protein polar localization. *Current Opinion in Plant Biology*, *53*, 134–140.

Rodriguez-Furlán, C., Minina, E. A., & Hicks, G. R. (2019). Remove, Recycle, Degrade: Regulating Plasma Membrane Protein Accumulation. *The Plant Cell*, *31*(12), 2833–2854.

Rodriguez-Furlán, C, Campos, R. C., Toth, J. N., & Van Norman, J. M. (2021). Distinct mechanisms underlie the contrasting polarity of IRK and KOIN, two LRR-RLKs involved in root tissue patterning [Manuscript submitted for publication].

Takano, J., Tanaka, M., Toyoda, A., Miwa, K., Kasai, K., Fuji, K., Onouchi, H., Naito, S., & Fujiwara, T. (2010). Polar localization and degradation of Arabidopsis boron transporters through distinct trafficking pathways.

Proceedings of the National Academy of Sciences of the United States of America, *107*(11), 5220–5225.

Tanaka, H., Nodzyłski, T., Kitakura, S., Feraru, M. I., Sasabe, M., Ishikawa, T., Kleine-Vehn, J., Kakimoto, T., & Friml, J. (2014). BEX1/ARF1A1C is required for BFA-sensitive recycling of PIN auxin transporters and auxin-mediated development in Arabidopsis. *Plant & Cell Physiology*, *55*(4), 737–749.

Van Norman, J. M. (2016). Asymmetry and cell polarity in root development. *Developmental Biology*, *419*(1), 165–174.

Van Norman, J. M., Zhang, J., Cazzonelli, C. I., Pogson, B. J., Harrison, P. J., Bugg, T. D. H., Chan, K. X., Thompson, A. J., & Benfey, P. N. (2014). Periodic root branching in Arabidopsis requires synthesis of an uncharacterized carotenoid derivative. *Proceedings of the National Academy of Sciences of the United States of America*, *111*(13), E1300–E1309.

Wysocka-Diller, J. W., Helariutta, Y., Fukaki, H., Malamy, J. E., & Benfey, P. N. (2000). Molecular analysis of SCARECROW function reveals a radial patterning mechanism common to root and shoot, *Development, 127*(3), 595–603

CHAPTER THREE: WFL polar localization in the epidermis is linked to its function in root hair positioning

ABSTRACT

As in other multicellular eukaryotic organisms, development of plant tissues and organs requires cellular communication. In Arabidopsis, polar accumulation of signaling proteins to specific plasma membrane domains provides positional information that informs developmental processes across cell types. Localization of polarly localized proteins often correlates with cellular function. Here we characterize the function of WALLFLOWER (WFL), a transmembrane receptor kinase that exhibits a dual polar localization in epidermal H cells, accumulating at the inner domain as well as at the root hair initiation domain. While *wfl* mutants don't have a detectable abnormal phenotype, overexpression of WFL leads to a downward shift in root hair (RH) position. This suggests WFL operates in a signaling pathway that functions across H cells to inform bulge position. RH position is unaffected upon deletion of WFL intracellular domains, indicating that the kinase domain is required to inform RH position. Roots overexpressing WFL-GFP are also sensitive to mechanical stress and prone to cell damage. However, this phenotype can be alleviated by cell wall rigidification or maintaining stable osmotic conditions. Together these observations suggest that WFL may have a role in coordinating cell wall modification with cellular expansion during RH development.

INTRODUCTION

With its well characterized cell types and predictable developmental events, the Arabidopsis root is an excellent model to study developmental processes in both space and time. The root is cylindrical in shape with tissues forming concentric layers around the central vasculature, and cells aligned into individual files in the longitudinal axis (Dolan et al., 1993). From the root tip shootward, development is elaborated in three zones: the cell division or meristematic zone, the zone of cell elongation, and finally, the maturation or differentiation zones (Benfey & Scheres, 2000). The well-defined cellular organization of the root allows for straightforward phenotypic analysis.

Cells are frequently partitioned into subdomains with unique features or functions and can therefore be described as polarized. Cell polarity can be defined as asymmetries in the localization of subcellular constituents and proteins and/or in cell morphology. In plants, one of the most dramatic examples of morphological polarity are root hairs (RHs). RHs are long tubular extensions of specialized epidermal cells called hair (H) cells and are an advantageous model for studies of polarity in development and how cellular polarity is achieved and maintained (Schiefelbein & Somerville, 1990). The formation of RHs during development of the root epidermis requires coordination between adjacent tissues and dramatic changes in subcellular and structural polarity to facilitate polarized cell growth.

Additionally, RHs increase root surface area and are functionally important for efficient uptake of water and nutrients and plant anchorage (Grierson et al., 2014).

RH initiation broadly occurs in two steps: initiation and tip growth through targeted secretion. During initiation, a small disc-shaped region of the cell wall located on the outer face towards the rootward end of epidermal H cells begins to soften and is called the RH initiation domain (RHID) (Grierson et al., 2014). One of the first proteins to arrive at the RHID is ROP GUANINE NUCLEOTIDE EXCHANGE FACTOR 3 (GEF3) followed by recruitment of RHO-RELATED PROTEIN FROM PLANTS 2 (ROP2) proteins (Denninger et al., 2019). Both GEF3 and ROP2 are uniformly distributed in the PM of these cells, but then accumulate specifically at the RHID. After establishment of the RHID, a bulge forms on the H cell surface followed by tip growth until the RH reaches its final length (Grierson et al., 2014).

Bulge formation and tip growth occur through intensive polarized secretion of cellular and cell wall materials to this specific region of the cell. Many proteins show higher accumulation at the growing tip of RHs; some of these proteins may be caught up in the bulk secretion scheme of RH elongation, but others, including many involved in signaling, are important for maintaining tip growth and cell wall integrity. For example, FERONIA (FER), a member of the Catharanthus roseus

RECEPTOR-LIKE KINASE 1-LIKE (CrRLK1L) subfamily of putative cell wall sensors, participates in many developmental processes, including vacuolar expansion for cell elongation (Dünser et al., 2019). In RH formation, FER forms a complex with ROPs and GEFs and regulates tip growth through accumulation of reactive oxygen species (ROS) at the RH tip. Loss of function of either FER or GEFs reduces ROS accumulation, resulting in RHs that are shorter than wild type (WT) and have abnormally shaped tips (Duan et al., 2010; Huang et al., 2013). Mutants of another, CrRLK1 related receptor, ERULUS (ERU), have a similar RH phenotype. ERU-GFP preferentially accumulates at the tip of the developing RH where it acts as a cell wall sensor protein that regulates cell wall elasticity through inhibition of pectin methylesterase activity (Kwon et al., 2018; Schoenaers et al., 2018). With the dramatic elongation of RHs, cell wall sensing is crucial to maintain cell wall integrity and prevent cell rupture and suggests that polar localization of receptors is important for normal RH formation.

In *Arabidopsis*, RH positioning is uniform and RHs emerge about 10 μm from the rootward edge of epidermal H cells with multiple factors informing position in the longitudinal axis (Grierson et al., 2014). *ROOT HAIR DEFECTIVE6* (*RHD6*) is a H cell-specific transcription factor and RHs of *rhd6* mutants are shifted toward the rootward edge of cells, suggesting that determination of RH position occurs early in RH development. This phenotype can be rescued by exogenous application of either auxin or ethylene, implicating a role for these plant hormones in RH

positioning (J. D. Masucci & Schiefelbein, 1994). Indeed, RH position is altered in auxin/ethylene perception and biosynthesis mutants (James D. Masucci & Schiefelbein, 1994; J. D. Masucci & Schiefelbein, 1996). Modification of cellular infrastructure is necessary to accommodate the drastic change in cellular polarity as a RH develops. Accordingly, RHs emerge in the middle of H cells when *ACTIN2* is mutated, indicating that the cytoskeleton is important for normal RH positioning (Ringli et al., 2002). Additionally, RHs in *procuste1* (*prc1-1*) mutants, which have a defect in the *CELLULOSE SYNTHASE6* (*CESA6*) gene, are shifted toward the rootward edge of H cells (Singh et al., 2008). As cellulose is the main load bearing component of the cell wall, these results indicate that that structural integrity also contributes to defining RH position.

Here we characterize the function of a polarly localized leucine-rich repeat receptor-like kinase (LRR-RLK) named WALLFLOWER (WFL). WFL specifically accumulates at the RHID and bulge of H cells and its polar localization appears to be linked to its function as overexpression perturbs RH position in the longitudinal axis, leading to a downward shift. Furthermore, overexpression of WFL lacking the intracellular domain does not alter RH position indicating that signal transduction or interaction with the kinase domain is likely required for this function. Additionally, WFL-GFP roots are sensitive to mechanical stress and prone to cell damage, however this phenotype can be alleviated by cell wall rigidification or maintaining stable osmotic conditions. Consistent with these

observations, WFL∆JxK-GFP roots are less sensitive to plasmolysis, implicating a role for WFL intracellular domains in osmotic sensing and/or stability. Thus, we propose WFL participates in a signaling pathway of polar growth at the epidermal surface, informing RH position.

RESULTS

Functional redundancy may account for the wild type phenotype of *wfl-1*

As shown in Chapter 2, we identified WFL, a LRR-RLK with polar localization in root epidermal cells and preferential localization in H cells. To understand the function of WFL in root development, a candidate insertational allele of *WFL* was obtained from the ABRC (Arabidopsis Resource Center), SAIL_1170_A12, but could not be used for any analyses in this paper as no heterozygous or homozygous mutant individuals could be identified. We then utilized CRISPR-Cas9 technology (Fauser et al., 2014) to generate *wfl* alleles. We identified *wfl-1,* which has reduced *WFL* expression (Figure 3.1) and has a single T insertion in the coding region of the second exon that results in a premature stop codon before the transmembrane domain. This suggests *wfl-1* is a null allele, because if a truncated protein was translated it would not be trafficked to the PM and is unlikely to be functional. We examined overall root length, average growth rate, and cellular morphology/patterning (not shown) in *wfl-1*, however, we could not detect any abnormal developmental phenotypes. These results suggest that

another or multiple closely related LRR-RLKs may be functionally redundant to WFL.

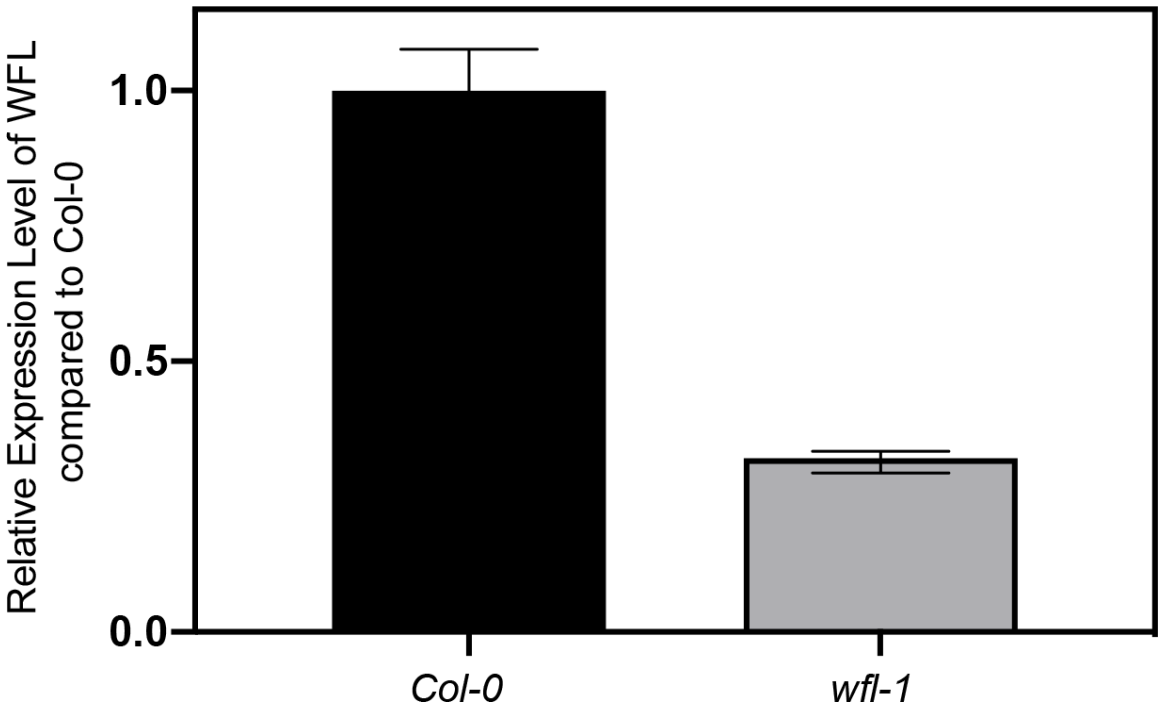

Figure 3.1. *WFL* transcript level is reduced in *wfl-1.*
RT-qPCR showed reduced *WFL* transcript levels in *wfl-1. WFL* expression is relative to *SERINE/THREONINE PROTEIN PHOSPHATASE2A* (*PP2A*). Data shown for one biological replicate (of three) with three technical replicates performed per experiment and each experiment was repeated three times. Error bars indicate standard error of the mean.

Within the RLK family of proteins, WFL is a member of subfamily LRR III which contains 35 members (S. H. Shiu & Bleecker, 2001; Shin Han Shiu & Bleecker, 2003). It is predicted that within the RLK family functional redundancy among closely related receptors is common (Diévart & Clark, 2003, 2004). We hypothesized that functional redundancy among WFL-related proteins may

account for the WT phenotype of *wfl-1* seedlings. We identified four of the most closely related receptors based on protein similarity and identity to WFL (Krogh et al., 2001; Möller et al., 2001; Sonnhammer et al., 1998) and obtained mutant alleles for each (Table 3.1). We first confirmed that all resultant progeny from these seeds were indeed homozygous for the mutant alleles and then crossed these WFL-related mutant alleles with our homozygous *wfl-1* mutant to generate double mutants. Double mutants are currently at the F2 generation and one individual homozygous for both alleles has been identified (*wfl-1, salk_005132*). Individuals heterozygous for *wfl-1* and WFL-related mutant alleles are currently at the F3 generation and genotyping for double mutants is ongoing. Future phenotypic analyses of double mutants may provide further insight into the functional role of WFL.

Gene ID	Protein % ID	Protein % Similarity	Mutant Allele
At5G53320	48.3%	61.5%	SALK_128780
At4G23740	47.6%	65.2%	SALK_005132
At5G01560	39.8%	57.5%	SALK_121868
At1G64210	44.3%	61.6%	SALK_200467C

Table 3.1: *WFL*-related genes and mutant alleles.
WFL-related proteins were chosen based on predicted protein identity and similarity. Mutant alleles were then obtained and used to generate double mutants with *wfl-1*.

WFL-GFP roots do not have a defect in cellulose biosynthesis

In Chapter 2 we mentioned that cell damage in *pWFL:WFL-GFP* expressing roots was alleviated by rigidifying the cell walls via a 24-hour exposure to -Pi growth conditions. These results suggest that this sensitivity may be a result of a cell wall defect and/or a defect in the relationship between the cell wall and the tonoplast of these transgenic plants. We first addressed the cell wall and examined the main load bearing component of the cell wall, cellulose (Cosgrove, 2005). To determine if there was a defect in cellulose synthesis, we treated WT and WFL-GFP roots with isoxaben, an inhibitor of cellulose biosynthesis. Treatment with isoxaben has been shown to induce cell damage as evidenced by PI penetration in cells (Chaudhary et al., 2020). We did not detect any difference between the two genotypes and observed a similar amount of PI penetration to cells (Figure 3.2). The cell wall is complex and structurally diverse and therefore, cellulose biosynthesis is not an exhaustive measure of cell wall integrity. Further experimentation will be required to determine if other cell wall components are impaired in WFL-GFP roots.

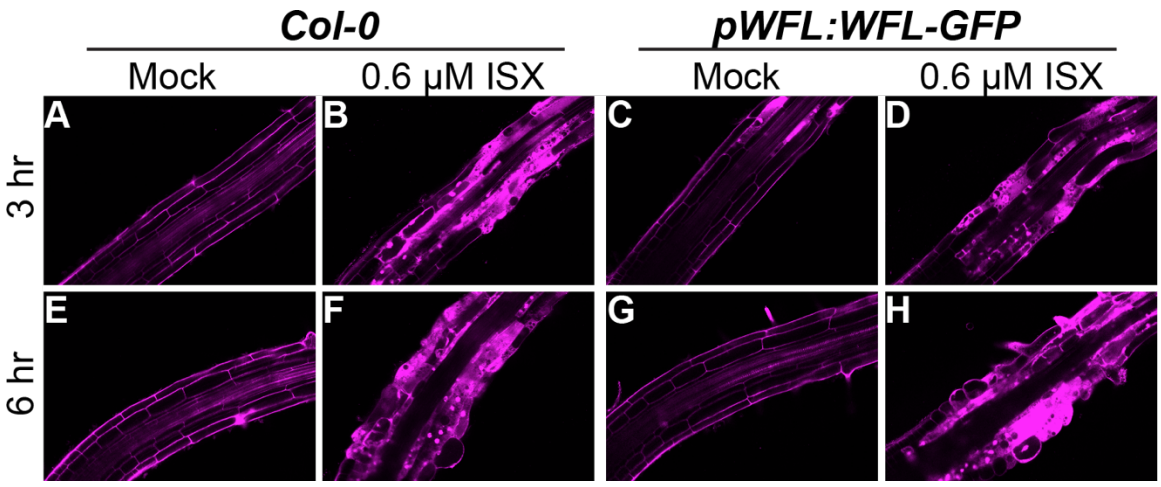

Figure 3.2: WFL-GFP roots do not have a defect in cellulose biosynthesis. (A-H) Confocal images of (A-B and E-F) WT and (C-D and G-H) WFL-GFP roots, stained with propidium iodide (PI) to show cell outlines. Adjacent panels show mock treated (left) and isoxaben treated (right) roots. PI penetration to cells is similar at 3 hr (A-D) and 6 hr (E-H) timepoints for both WT and WFL-GFP roots.

WFL kinase domain is important for cell turgor maintenance

Turgor pressure is the force exerted on the plasma membrane and cell wall by water passing into the cell by osmosis and is the driving force for wall deformation (Cosgrove, 2005). Therefore, constant maintenance of turgor pressure is important for normal growth and development of plant cells. We observed that maintaining stable osmotic conditions alleviated cell damage when imaging WFL-GFP roots. Roots mounted on slides with 1x liquid MS, as opposed to water, were less susceptible to cell damage (not shown). We hypothesized that a defect in turgor maintenance may be the causal factor for the observed cell damage. To test this we first selected a PM marker line to use as a control. We examined root cell plasmolysis of two different PM marker lines (*p35S:FH6-GFP* and *pUBQ10:WAVE131-YFP),* at two different concentrations of mannitol (0.4 M

and 0.6 M). To quantify plasmolysis we categorized roots as either plasmolyzed or partially plasmolyzed. For an individual root to be counted as a plasmolyzed root, the PM was completely separated from the cell wall at each corner in the majority of epidermal cells observed; whereas for partially plasmolyzed roots, the PM was still attached to at least one corner of the majority of epidermal cells observed. We observed no differences between the two reporter lines and moved forward with FH6-GFP roots as our control.

We then compared root plasmolysis between WFL-GFP and FH6-GFP and observed no difference between the two genotypes at either concentration of mannitol (Figure 3.3A-B, D-E, and G), suggesting that there is no turgor defect in WFL-GFP roots. We observe that unlike WFL-GFP roots, WFL∆JxK-GFP roots are not sensitive to osmotic or mechanical stress. Therefore, we examined their response to plasmolysis conditions and, unexpectedly, found that WFL∆JxK-GFP roots were less sensitive to plasmolysis conditions than either FH6-GFP and WFL-GFP roots (Figure 3.3C, F-G). These results indicate that WFL intracellular domains are important to inform turgor pressure across the cell, and suggest that despite a normal response to plasmolysis when WFL is overexpressed, WFL may have a role in turgor pressure maintenance.

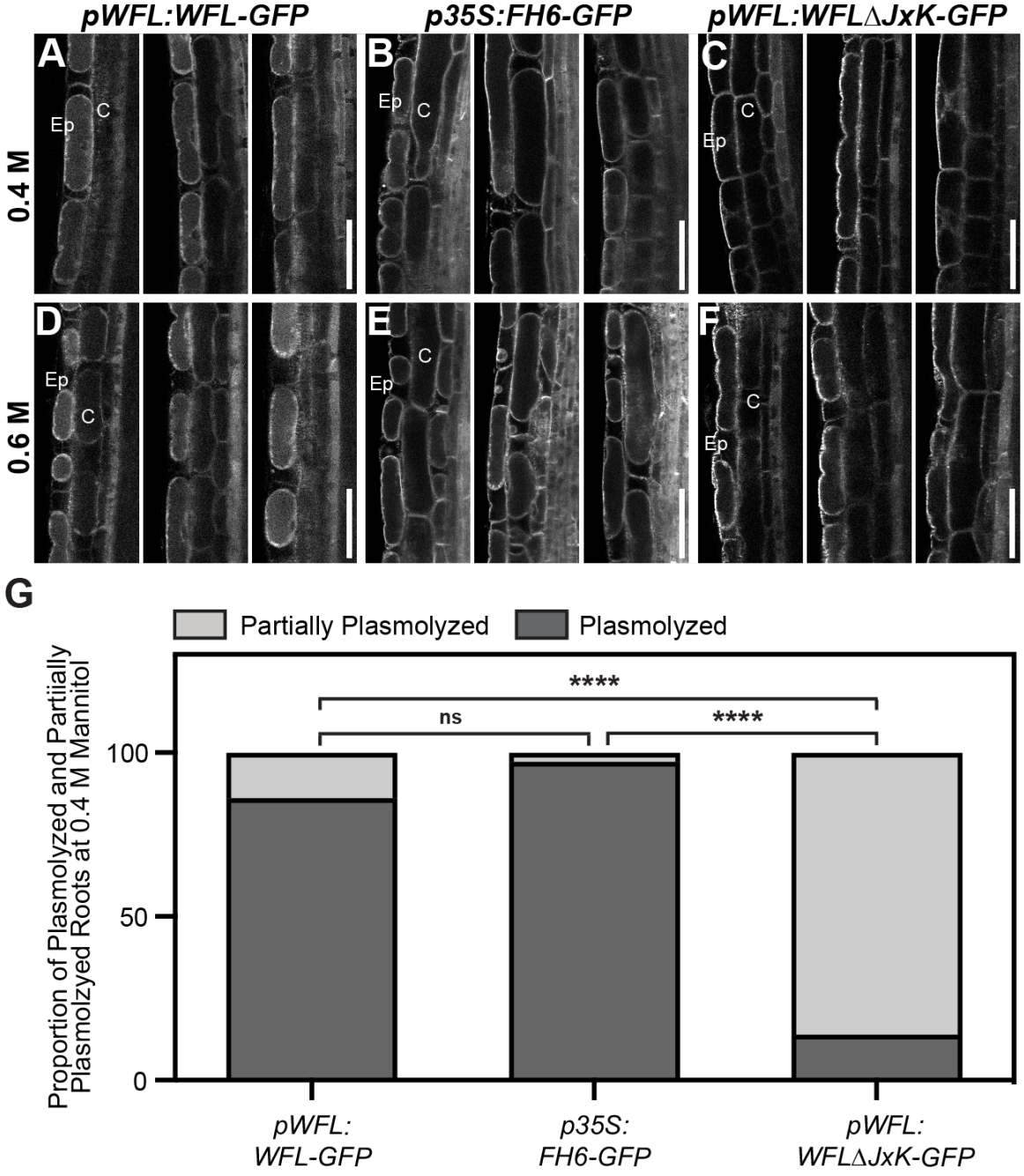
pWFL:WFL-GFP
p35S:FH6-GFP
pWFL:WFLΔJxK-GFP
A
B
C
D
E
F
Ep
C
0.4 M
0.6 M
G
Partially Plasmolyzed
Plasmolyzed
Proportion of Plasmolyzed and Partiially Plasmolzyed Roots at 0.4 M Mannitol
****
ns
****
100
50
0
pWFL: WFL-GFP
p35S: FH6-GFP
pWFL: WFLΔJxK-GFP

Figure 3.3: WFL intracellular domains are important for normal turgor maintenance in epidermal cells.
(A-F) Representative confocal images of cell plasmolysis at (A-C) 0.4 M and (D-F) 0.6 M mannitol in roots expressing (A and D) *pWFL:WFL-GFP,* (B and E) *p35S:FH6-GFP,* and (C and F) *pWFL:WFLΔJxK-GFP.* (G) Roots were categorized as either plasmolyzed or partially plasmolyzed based on the number of plasmolyzed epidermal cells. Roots expressing (A and D) *pWFL:WFL-GFP* and (B and E) *p35S:FH6-GFP* responded similarly to plasmolysis by treatment with both mannitol concentrations. In contrast, roots expressing (C and F) *pWFL:WFLΔJxK-GFP* were less sensitive (C and F). For graph: student's t test, **** $p<0.0001$. Data shown is representative of all data for 3 biological replicates, with n=12 roots and 5 cells per root for each replicate. Abbreviations: Ep, Epidermis; C, Cortex. Scale bars: 25 μm.

Overexpression of WFL affects the position of RHIDs and RH bulges

In roots overexpressing WFL-GFP, we also observed that RH position is perturbed. In WT plants the RHID is normally located approximately 10 μm from the rootward edge of epidermal H cells (Figure 3.4A, Grierson et al., 2014). However, in *pWFL:WFL-GFP* roots, we observed that bulge formation is shifted downward toward the rootward edge of H cells (Figure 3.4B). To quantify this phenotype we classified RH bulge position as WT (normal) or shifted downward, where shifted RHs have no measurable distance between the RH bulge and the rootward edge of the cell. We used confocal microscopy to quantify bulge position in two independent *pWFL:WFL-GFP* transgenic lines and concluded that bulge position is indeed shifted towards the rootward edge of H cells in these roots (Figure 3.4D). These results indicate that overexpression of WFL-GFP in a WT background leads to a defect in RH positioning.

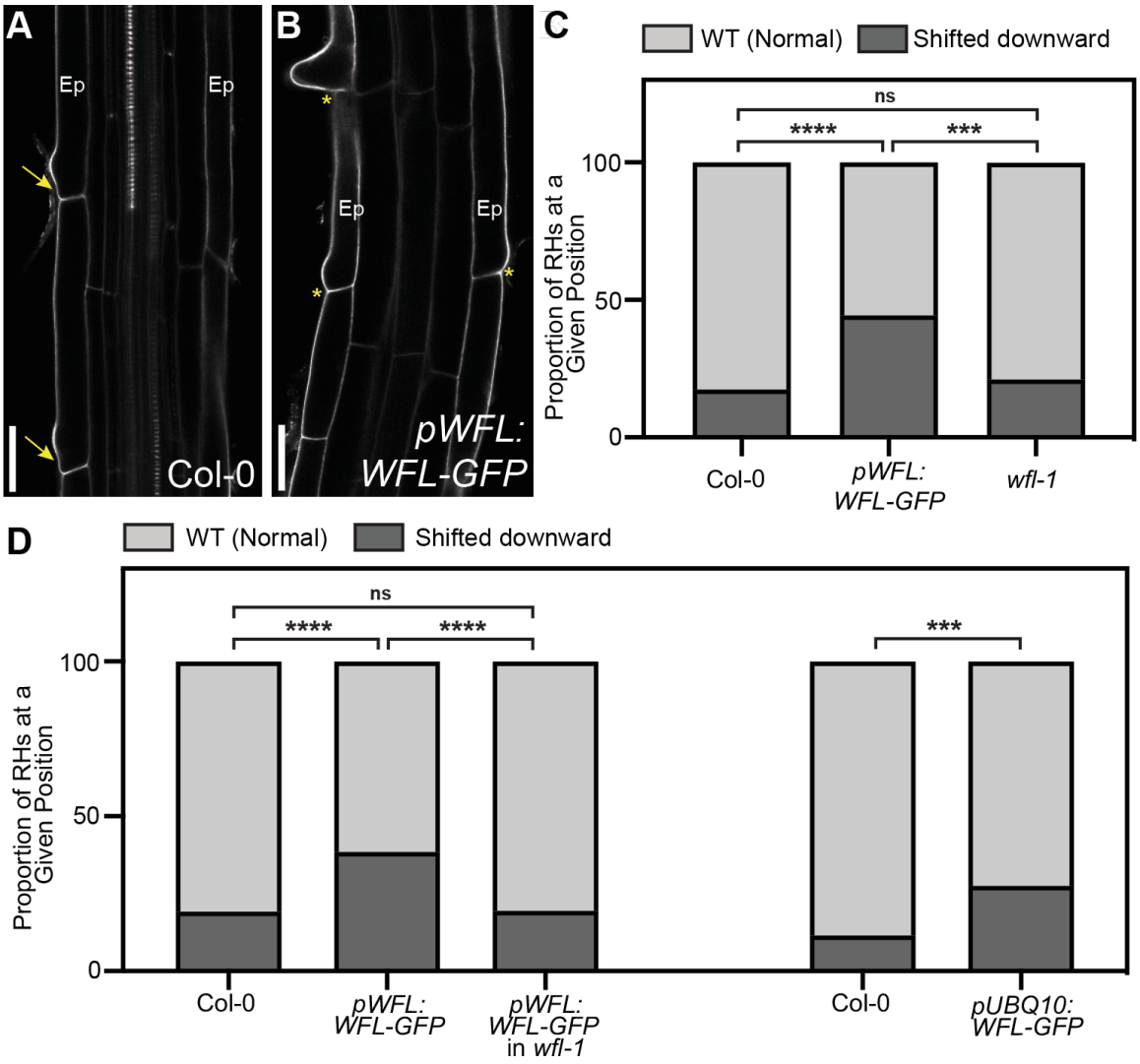
A
Ep
Ep
Col-0
B
Ep
Ep
pWFL:
WFL-GFP
C
WT (Normal)
Shifted downward
ns
****
***
100
50
0
Proportion of RHs at a Given Position
Col-0
pWFL:
WFL-GFP
wfl-1
D
WT (Normal)
Shifted downward
ns
****
****
***
100
50
0
Proportion of RHs at a Given Position
Col-0
pWFL:
WFL-GFP
pWFL:
WFL-GFP
in wfl-1
Col-0
pUBQ10:
WFL-GFP

Figure 3.4: Overexpression of WFL-GFP shifts RH position downward toward the rootward edge of H cells.
(A and B) Confocal images showing propidium iodide (PI) stain (gray) to show cell outlines of (A) WT and (B) WT roots expressing *pWFL:WFL-GFP*. (A) RHs in WT roots have a defined space between the rootward edge of H cells and the site of the RH bulge (yellow arrows). (B) In contrast, in roots expressing *pWFL:WFL-GFP,* RHs are shifted downward towards the rootward edge of H cells (yellow asterisks). (C and D) RHs were binned into 2 categories based on position and quantified according to genotype. (C) RH bulge position in *wfl-1* and WT is the same, whereas RH bulges are shifted downwards when WFL-GFP is overexpressed by either *pWFL* or (D) *pUBQ10*. (D) No change in RH bulge position is observed when *pWFL:WFL-GFP* is expressed in *wfl-1*. For graphs: student's t test, *** $p<0.001$ and **** $p<0.0001$. Data shown is from one (of two) independent transgenic lines per reporter (with similar results for each line in each replicate) and 3-4 biological replicates combined, with n=15 roots and 3-5 cells per root per replicate. Abbreviations: Ep, Epidermis. Scale bars: 25 μm.

To confirm the level of *WFL* overexpression in *pWFL:WFL-GFP* transgenic plants compared to non-transgenic WT controls, we conducted RT-qPCR. *WFL* transcript levels were ~2-fold higher in transgenic plants compared to WT and were similar between the two independent transgenic lines (Figure 3.5B). Additionally, when bulge position was quantified in another overexpression line where WFL-GFP is expressed from under the control of the constitutively active *UBIQUITIN10* promoter (*pUBQ10, pUBQ10:WFL-GFP*) we observed that bulges are shifted downward (Figure 3.4D). Notably, the proportion of shifted bulges in *pUBQ10:WFL-GFP* roots was similar to that of *pWFL:WFL-GFP* roots confirming the relationship between WFL overexpression and altered RH positioning. These results suggest overexpression (above the endogenous level) or increased copy number of WFL leads to a shift in RH position, however, an alternative explanation is that GFP somehow interferes with WFL function causing this phenotype. To ensure that the GFP tag was not contributing to alter RH bulge position, we generated an untagged version of the transgene (*pWFL:WFL*) and upon its expression in WT, observed a similar shift in RH bulge position as seen in WFL-GFP fusions (Figure 3.5A). Thus, the fusion of GFP to WFL cannot explain the abnormal RH bulge position phenotype, supporting the conclusion that expression level or increased copy number leads to this phenotype.

Given this overexpression phenotype, we reexamined *wfl-1* and did not observe any RH positioning phenotype (Figure 3.4C). Furthermore, expression of

pWFL:WFL-GFP in the *wfl-1* background did not result in a shift in the position of RH bulges (Figure 3.4D) indicating a reduction in expression or functional copy number alleviates this phenotype. Finally, we examined RH bulge position in WT and *wfl-1* roots expressing *pWFL:WFL*Δ*JxK-GFP* and found that bulge position was unaffected in either genotype (Figure 3.5C). Taken together, these results indicate that only expression of full length WFL above the endogenous level elicits a shift in RH bulges toward the rootward edge of H cells indicating that the WFL intracellular domains and/or subcellular localization are required for this phenotype.

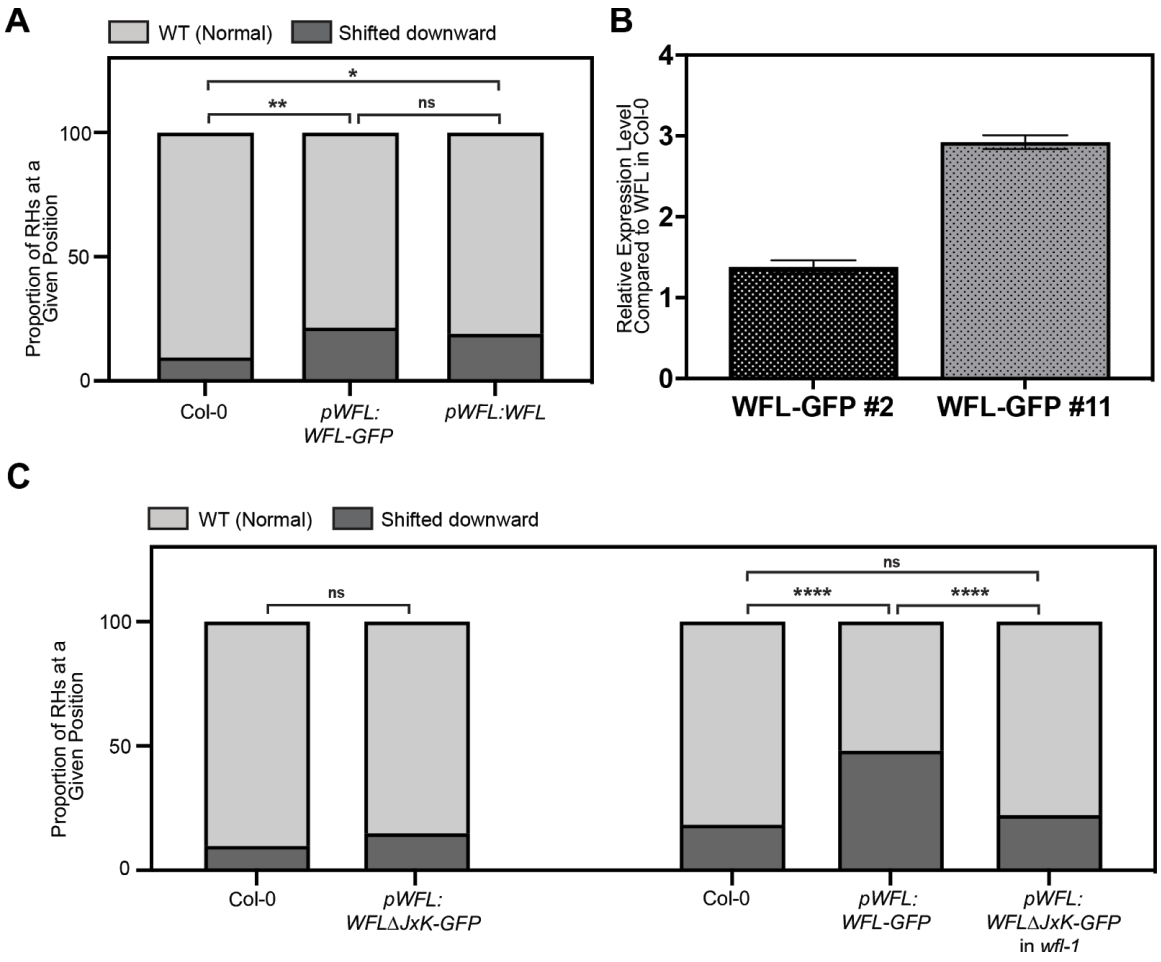

Figure 3.5: GFP does not cause shifted RH bulge phenotype and this phenotype is not observed in roots expressing *pWFL:WFLJxK-GFP*.(A and C) RH bulges were binned into two categories and quantified according to genotype. (A) RH bulges are shifted towards the rootward edge of H cells in roots expressing an untagged version of WFL (*pWFL:WFL*). (C) Bulge position is unaffected in roots expressing *pWFL:WFLΔJxK-GFP* and *pWFL:WFLΔJxK-GFP* in *wfl-1*. (B) RT-qPCR showing transcript levels of *WFL* among transgenic lines used for phenotyping. Error bars show standard error of the mean. For RH bulge position graphs: student's t test, *p<0.05, ** p<0.01 and **** p<0.0001. Data shown is from one (of two) independent transgenic lines per reporter (with similar results for each line in each replicate) and 2-3 biological replicates combined, with n= 15 roots and 3-5 cells per root per replicate.

DISCUSSION

WFL is a member of the largest gene family in Arabidopsis, the receptor-like kinases (RLKs), and belongs to the largest group of receptors, LRR-RLKs. Within LRR-RLKs, there is predicted functional redundancy among closely related receptors, and therefore, phenotypes are often difficult to identify in single mutants (Diévart & Clark, 2003, 2004). We were unable to identify an abnormal phenotype in *wfl-1,* suggesting that, in the absence of WFL, another closely related LRR-RLK may be sufficient for normal function. While *wfl-1* is phenotypically wild type, we observed that overexpression of WFL results in a shift in RH position downward toward the rootward edge of H cells. In contrast, RHs are not shifted in WFLΔJxK-GFP roots, indicating that WFL intracellular domains are necessary for this phenotype. In addition to shifted RHs, we also observe that WFL-GFP roots are sensitive to mechanical stress and that this sensitivity can be alleviated by exposure to -Pi growth conditions, which rigidifies cell walls in root cells. This suggests WFL overexpression may lead to alterations in the cell wall itself or may disrupt interactions between the tonoplast and the cell wall. Intriguingly, WFL localizes to areas of the root where dramatic changes to the cell wall are taking place, including the outermost layer of the LRC, the elongation zone, and RHIDs and bulges. The presence of WFL at these positions of cell wall modification together with a shifted RH position upon WFL overexpression of WFL-GFP make it very tempting to speculate that WFL is involved in cell wall modification.

In further support of a role for WFL in cell wall modification, the Search Tool for the Retrieval of Interacting Genes/Proteins (STRING) database predicts interactions with a RH-specific proline-rich extensin-like family protein (EXT15, AT1G23720) and two RH-specific Class III (CIII) peroxidase (PRX) proteins (PRX27, AT3G01190 and PRX57, AT5G17820) ((Szklarczyk et al., 2019). *prx57* mutants have shorter RHs with extensive rupturing, indicating that PRX57 plays a role in cell wall modification during RH elongation (Kwon et al., 2015). It is known that LRR-RLKs interact with extensins, for example, FERONIA is known to interact with LEUCINE-RICH REPEAT/EXTENSIN 1 (LRX1) to coordinate cell wall loosening with cell elongation (Dünser et al., 2019). Future research into a possible role for WFL in cell wall modification through these cell wall-associated proteins and their potential interaction with WFL are intriguing areas for future study.

Furthermore, in *procuste1* mutants, which have a defect in the *CELLULOSE SYNTHASE6* (*CESA6*) gene, RH position is shifted toward the rootward edge of H cells, similar to the phenotype observed in roots overexpressing WFL-GFP (Singh et al., 2008). Cellulose provides structural support for the main plant body and is the main load-bearing component of the cell wall (Cosgrove, 2005). We treated WFL-GFP roots with isoxaben to examine the effects of a defect in cellulose biosynthesis, but did not observe a difference from WT. These results indicate that WFL-GFP roots do not have a defect in cellulose biosynthesis.

However, the cell wall is structurally complex and WFL may regulate another cell wall component or may be involved in maintaining other components of cellular infrastructure to inform RH position.

Modification of cellular infrastructure is required to accommodate the drastic change in cellular polarity as a RH develops and, therefore, there are multiple factors that influence RH position. In the *deformed root hairs 1* mutant, in which *ACTIN2* is mutated, RHs often emerge in the middle of H cells, indicating that the cytoskeleton is important for proper bulge formation (Ringli et al., 2002). Hormones also have a role in determining RH position, as positioning is affected in auxin/ethylene perception and biosynthesis mutants (James D. Masucci & Schiefelbein, 1994; J. D. Masucci & Schiefelbein, 1996). Additionally, during RH development, coordination of turgor pressure with the growing cell wall is critical to accommodate the rapidly expanding cell. The main driver of cellular expansion is turgor pressure (Mendrinna & Persson, 2015) and cell turgor is regulated by sensing changes in osmolarity (Grierson et al., 2014). Upon treatment with mannitol, we observed no difference in cell plasmolysis between our control, FH6-GFP, and WFL-GFP roots. However, WFLΔJxK-GFP roots appeared to be less sensitive to plasmolysis compared to our control, suggesting that WFL intracellular domains are important for normal cell turgor maintenance. Furthermore, we observed that RHs are not shifted in WFLΔJxK-GFP roots, indicating that WFL intracellular domains are required for the shifted RH

phenotype in WFL-GFP roots. Thus, it is possible that during RH bulge formation WFL intracellular domains coordinate turgor pressure and the expanding cell wall, and upon overexpression this communication/signaling is disrupted, resulting in misplacement of the RH.

While a definitive mechanism for WFL function remains elusive, our data are consistent with its function in cell wall modification during development. Our observations demonstrate that WFL is a polarly localized LRR-RLK with unique localization in H cells that is linked to its function in RH positioning. It is also clear that WFL intracellular domains are functionally important for RH positioning, as only overexpression of the full length protein results in a shift in RH position. We propose that the specific localization of WFL to RHIDs and bulges is linked to WFL function and that overexpression affects normal RH positioning in the longitudinal axis. The shift in RH position together with sensitivity to mechanical and osmotic stress in WFL-GFP roots make it tempting to speculate that WFL may have a functional role in cell wall integrity and/or cell turgor maintenance. Further research will be required to understand precisely how WFL influences cellular processes throughout RH development.

MATERIALS AND METHODS

Plant materials and growth conditions

The *Arabidopsis thaliana* Columbia-0 accession was used as the wild type. Standard growth media consisted of 0.5x or 1x Murashige and Skoog (MS) salts (Caisson labs), 0.5 g/L MES (EMD), 1% sucrose, pH 5.7, and 1% agar (Difco), unless otherwise noted. Seeds were surface sterilized with chlorine gas, stratified in tubes at 4°C for 2-3 days and then plated on 100 mm plates with standard growth medium. Plates were then placed vertically in a Percival incubator under long day conditions (16 h light/8 h dark) at a constant temperature of 22°C. Plates were sealed with parafilm for experimental analyses. Seedlings were typically examined between 4-7 days post-stratification (dps). Details for individual experiments are listed in figure legends and/or below.

A candidate insertational allele of *WFL* was obtained from the ABRC (Arabidopsis Resource Center), SAIL_1170_A12, but could not be used for any analyses in this disseration as no heterozygous or homozygous mutant individuals could be identified. An allele (*wfl-1*) was generated using CRISPR-Cas9 technology and used for all phenotypic analyses.

Insertional alleles for WFL-related genes were obtained from the ABRC (listed in Table 3.1). Resultant progeny were genotyped and confirmed to be homozygous

(primers are listed in Table 3.2). To generate double mutants, plants homozygous for individual WFL-related mutant alleles were then crossed to homozygous *wfl-1* plants. Heterozygous F1 plants were allowed to self and the resultant segregating F2 generation was genotyped to identify double mutants. If we were unable to identify a double mutant in the F2 generation, we selected individuals from the F2 that were homozygous for one allele and heterozygous for the other and collected F3 seeds for further genotyping. Double mutant identification in F3 plants is ongoing and progeny will be used to generate triple mutants for future analyses.

Vector Construction and Plant Transformation

Transcriptional and translational reporter genes were constructed by standard molecular biology methods and utilizing Invitrogen Multisite Gateway® technology (Carlsbad, USA). A region 4.1 kb upstream of the *WFL* (At5g24100) start codon was amplified from Col-0 genomic DNA and recombined into the Invitrogen pENTR™ 5'-TOPO® TA vector. For translational fusions, the genomic fragment encoding *WFL* from the ATG up to, but excluding the stop codon (including introns, 2.0 kb), was amplified from Col-0 genomic DNA and recombined into the Invitrogen pENTR™ DIRECTIONAL TOPO® (pENTR-D-TOPO) vector and fused to a C-terminal GFP tag (unless otherwise noted) as previously described (Van Norman et al., 2014). Specific primers for *WFL* cloning are listed in Table 3.3.

WFL-GFP was overexpressed using *pUBQ10* as previously described (Campos et al., 2020; Lee et al., 2006). The various Gateway compatible fragments were recombined together with the dpGreen-BarT or dpGreen-NorfT destination vector (Lee et al., 2006).

The dpGreenNorfT was generated by combining the backbone of dpGreenBarT with the p35S::tpCRT1 and terminator insert from pGII0125. Within the target region of the dpGreenBarT, one AclI site was mutated with the QuickChangeXL kit (Stratagene). Plasmids were amplified in ccdB-resistant E.coli and plasmids prepped with a Bio Basic Plasmid DNA Miniprep kit. 34uL of the modified dpGreenBarT and unmodified pGII0125 were digested with 1ul each FspI and AclI in CutSmart buffer (NEB) for 1hr at 37C. Digests were subjected to gel electrophoresis on a 1% agarose gel. The 5866bp fragment from the dpGreenBarT and 2592bp fragment from the pGIII0125 were extracted with a Qiagen MinElute Gel Extraction kit. The fragments were then ligated at 1:1 volumetric ratio (20ng vector; 8.8ng insert) using T4 DNA ligase incubated at 16C overnight before transformation into ccdB-resistant E.coli.

Expression constructs were then transformed into Col-0 plants by the floral dip method (Clough & Bent, 1998) using Agrobacterium strain GV3101 (Koncz et al., 1992) and transformants were identified using standard methods. For each

reporter gene, T2 lines with a 3:1 ratio of resistant to sensitive seedlings, indicating the transgene is inherited as a single locus, were selected for propagation. These T2 plants were allowed to self and among the subsequent T3 progeny, those with 100% resistant seedlings, indicating that the transgene was homozygous, were used in further analyses.

CRISPR-induced mutagenesis was performed as described in (Fauser et al., 2014), a single guide RNA (5'-TTTAACGGTAGTATTCCCGCGGG) was selected in exon 2 of *WFL.* T2 lines that exhibited a 3:1 ratio of resistant to sensitive seedlings, indicating the CRISPR-guideRNA-containing transgene was inherited as a single locus, were selected for continued analyses and sensitive plants were transferred to 1X MS standard growth media to recover. These plants were subsequently tested for lesions in *WFL* in proximity to the guideRNA binding site. We identified *wfl-1,* which has reduced *WFL* expression (Figure 3.1) and has a single T insertion in the coding region of the second exon that results in a premature stop codon before the transmembrane domain.

Phenotypic analyses

Root hair bulge position measurement protocol was modified from that was previously described in (J. D. Masucci & Schiefelbein, 1994). For root hair bulge position quantification ~15 roots of each genotype were grown side-by-side on 0.5x MS plates until 4 dps. To image roots, seedlings were stained with ~10 μM

propidium iodide (PI) solubilized in water for 1-2 min and visualized via laser scanning confocal microscopy on a Leica SP8 upright microscope housed in the Van Norman lab. For each biological replicate, imaging was done in median longitudinal sections at the beginning of the differentiation zone of 15 roots with 5-6 epidermal cells with a root hair bulge selected from each root for analysis. Root hair bulges were binned into 2 categories with the following parameters: “normal (WT)” if there was a measurable distance from the emerging root hair to the rootward edge of the cell and “shifted” if there was no measurable distance. Images were analyzed using ImageJ software for at least 2-3 biological replicates analyzed for each genotype.

The cell damage protocol was modified from those previously described in (Chaudhary et al., 2020). Seedlings were grown vertically and side-by-side on 1X MS plates until 7 dps. Individual seedlings were transferred into liquid 1X MS media containing either 0.01 percent methanol (mock) or 600 nM isoxaben and incubated for 3 or 6 hours. To image roots, seedlings were stained with PI (as described above) and imaged using confocal microscopy. Images were acquired at each time point. Cell damage was assessed based on PI penetration to individual cells. Images were reviewed using ImageJ software for each of 2 biological replicates.

For plasmolysis experiments, 4-5 cells from 12 individual roots of each genotype were treated with 2 different Mannitol (Difco, Cat# 217020) concentrations (0.4 M and 0.6 M). Roots were incubated in either 1x MS + 0.4 M or 1x MS + 0.6 M mannitol for 15 minutes And then imaged using confocal microscopy. Root plasmolysis was determined based on PM detachment from cell corners, and roots were categorized as either plasmolyzed or partially plasmolyzed. In plasmolyzed roots, the PM was completely separated from the each of the 4 corners of the cell in at least 5 epidermal cells; and in partially plasmolyzed roots, cells remained attached to at least 1 cell corner in at least 5 epidermal cells. Images were analyzed using ImageJ software for at least 3 biological replicates analyzed for each genotype.

RT-qPCR analysis

Total RNA for quantitative RT-PCR (qRT-PCR) was isolated using Qiagen's RNeasy Plant Mini Kit. Total RNA was extracted from whole seedlings at 7 dps after growth on our standard 1X MS (*wfl-1* and Col-0*)* or 0.5x MS (Col-0 and *pWFL:WFL-GFP)* growth medium and sealed with parafilm. For each of the biological replicates Col-0 and *wfl-1* or *pWFL:WFL-GFP* were grown side-by-side on the same plate. RNA was isolated for three independent biological replicates for Col-0, *pWFL:WFL-GFP,* and the *wfl-1* allele. First-strand cDNA was synthesized from 1 µg total RNA with RevertAid First Strand cDNA Synthesis and the oligo$(dT)_{18}$ primer (Thermo Scientific). qRT-PCR reactions were set up using

IQ SYBR Green Supermix (BioRad) and analysis was performed on the CFX-Connect Real-Time System housed in the Integrative Institute of Genome Biology Genomics Core facility at UC-Riverside. The reaction conditions for each primer pair were: 95°C for 3 min followed by 40 cycles of 95°C for 10s and 57°C for 20 s. Standard curves were performed at least in duplicate. Primer pair efficiency values were calculated for each replicate of the standard curves and the average efficiency was used for subsequent analysis (Table 3.4). For each genotype and biological replicate, three technical replicates were performed. Data analysis was performed with the Bio-Rad CFX Manager software 3.1 and transcript levels were normalized to *SERINE/THREONINE PROTEIN PHOSPHATASE2A* (*PP2A) (*Czechowski et al., 2005*)*.

Quantification and statistical analysis

The Leica LAS X software, as well as ImageJ were used for post-acquisition confocal image processing. Graphs were generated using PRISM8 (GraphPad Software, https://www.graphpad.com/, San Diego, USA). Microsoft Excel was used for student's t tests. The exact value of n, what n represents, the number of biological or technical replicates, the means, and standard error of the mean (SEM) are indicated in each of the relevant figure legends and/or in tables.

Mutant Allele	Reaction Type	F Primer Name	F Primer Seq (5'->3')	R Primer name	R Primer Seq (5'->3')
SALK_128780	WT	128780_LP	ATGCATCAGTGTAGCCATTCC	128780_RP	CTCGACTTCAACGAGTTTTCG
	Mutant	LBb1.3	ATTTTGCCGATTTCGGAAC		
SALK_005132	WT	005132_LP	AAGCTCCACAACGTTTTCATG	005132_RP	ATGCAACCAACTCGTTCACTC
	Mutant	Lbal	TGGTTCACGTAGTGGGCCATCG		
SALK_121868	WT	121868_LP	GTAACATTCCTTCCGGTCTCC	121868_RP	GAGTTAAAGGTGTCTTCCCGG
	Mutant	LBb1.3	ATTTTGCCGATTTCGGAAC		
SALK_200467C	WT	200467C_LP	TCATAGCTGGACCGGTGTTAC	200467C_RP	TGTATGAACTTCCCTTCGTGG
	Mutant	LBb1.3	ATTTTGCCGATTTCGGAAC	200467C_LP	TCATAGCTGGACCGGTGTTAC

Table 3.2. *WFL*-related mutant alleles and associated genotyping primers.

Purpose	Primer Name	Sequence (5'->3')
Genotyping	WFLcod_seqF3*	GGTACTATCAGCCGTCTATCG
	WFLcod_seqR2*	ATTTCGCTCTTATCCTCCATGTC
	*The amplicon generated by these primers needs to be digested with SacII for genotyping	
Cloning	WFLcod_F	caccATGAGTAGAGGAAGATCTTTCATCTTC
	WFLcod_R	GTCTCTCTCAATCTCTTCCAAAGTC
	WFLpro_F	CGAAGAGTCATGTTGGTCATGTT
	WFLpro_R	CTTCTTACTAATTGTTATGTGATGGA
	WFLcod_truncR	TGTCTCTGACTTCCTCTGCCT
	WFLcod_trunc-K_R	TGCAGAAGCTATCAACAAGTCTTC

Table 3.3. Cloning and genotyping primers related to Figures 3.1-3.5.

		Primer Efficiency (%)					
Primer Name	**Primer Sequence (5'->3')**	**Run 1**	**Run 2**	**Run 3**	**Run 4**	**Run 5**	**Average**
PP2A_qF	TAACGTGGCCAAAATGATGC	88.1%	96%	95.8%	90.1%	97.9%	93.6%
PP2A_qR	GTTCTCCACAACCGCTTGGT						
WFL_ex1/2_qF	CGCATTTGAACTATATAAAAGTC	91.2%	77.9%	91.3%	82.5%	104.6%	89.5%
WFL_ex2_qR2	ACAGAGCCGATGATCCAAAGA						
WFL_ex2_qF3	GCTTACGTGTGTTCCAAGGA	92.9%	91.3%	ND	ND	ND	92.1%
WFL_ex2/3_qR1	GTCTGCGTTCTTGCCATGAA						

Table 3.4. Primers and primer efficiency information for RT-qPCR, related to Figures 3.1 and 3.5.

REFERENCES

Benfey, P. N., & Scheres, B. (2000). Root development. *Current Biology: CB*, *10*(22), R813–R815.

Campos, R., Goff, J., Rodriguez-Furlán, C., & Van Norman, J. M. (2020). The Arabidopsis Receptor Kinase IRK Is Polarized and Represses Specific Cell Divisions in Roots. *Developmental Cell*, *52*(2), 183–195.e4.

Chaudhary, A., Chen, X., Gao, J., Leśniewska, B., Hammerl, R., Dawid, C., & Schneitz, K. (2020). The Arabidopsis receptor kinase STRUBBELIG regulates the response to cellulose deficiency. *PLoS Genetics*, *16*(1), e1008433.

Clough, S. J., & Bent, A. F. (1998). Floral dip: a simplified method for Agrobacterium-mediated transformation of Arabidopsis thaliana. *The Plant Journal: For Cell and Molecular Biology*, *16*(6), 735–743.

Cosgrove, D. J. (2005). Growth of the plant cell wall. *Nature Reviews. Molecular Cell Biology*, *6*(11), 850–861.

Czechowski, T., Stitt, M., Altmann, T., Udvardi, M. K., & Scheible, W.-R. (2005). Genome-wide identification and testing of superior reference genes for transcript normalization in Arabidopsis. *Plant Physiology*, *139*(1), 5–17.

Denninger, P., Reichelt, A., Schmidt, V. A. F., Mehlhorn, D. G., Asseck, L. Y., Stanley, C. E., Keinath, N. F., Evers, J.-F., Grefen, C., & Grossmann, G. (2019). Distinct RopGEFs Successively Drive Polarization and Outgrowth of Root Hairs. *Current Biology: CB*, *29*(11), 1854–1865.e5.

Diévart, A., & Clark, S. E. (2003). Using mutant alleles to determine the structure and function of leucine-rich repeat receptor-like kinases. *Current Opinion in Plant Biology*, *6*(5), 507–516.

Diévart, A., & Clark, S. E. (2004). LRR-containing receptors regulating plant development and defense. *Development* , *131*(2), 251–261.

Dolan, L., Janmaat, K., Willemsen, V., Linstead, P., Poethig, S., Roberts, K., & Scheres, B. (1993). Cellular organisation of the Arabidopsis thaliana root. *Development* , *119*, 71–84.

Duan, Q., Kita, D., Li, C., Cheung, A. Y., & Wu, H.-M. (2010). FERONIA receptor-like kinase regulates RHO GTPase signaling of root hair development. *Proceedings of the National Academy of Sciences of the United States of America*, *107*(41), 17821–17826.

Dünser, K., Gupta, S., Herger, A., Feraru, M. I., Ringli, C., & Kleine-Vehn, J. (2019). Extracellular matrix sensing by FERONIA and Leucine-Rich Repeat Extensins controls vacuolar expansion during cellular elongation in Arabidopsis thaliana. *The EMBO Journal*, *38*(7). https://doi.org/10.15252/embj.2018100353

Fauser, F., Schiml, S., & Puchta, H. (2014). Both CRISPR/Cas-based nucleases and nickases can be used efficiently for genome engineering in Arabidopsis thaliana. *The Plant Journal: For Cell and Molecular Biology*, *79*(2), 348–359.

Grierson, C., Nielsen, E., Ketelaarc, T., & Schiefelbein, J. (2014). Root hairs. *The Arabidopsis Book / American Society of Plant Biologists*, *12*, e0172.

Huang, G.-Q., Li, E., Ge, F.-R., Li, S., Wang, Q., Zhang, C.-Q., & Zhang, Y. (2013). Arabidopsis RopGEF4 and RopGEF10 are important for FERONIA-mediated developmental but not environmental regulation of root hair growth. *The New Phytologist*, *200*(4), 1089–1101.

Koncz, C., Németh, K., Rédei, G. P., & Schell, J. (1992). T-DNA insertional mutagenesis in Arabidopsis. *Plant Molecular Biology*, *20*(5), 963–976.

Krogh, A., Larsson, B., von Heijne, G., & Sonnhammer, E. L. (2001). Predicting transmembrane protein topology with a hidden Markov model: application to complete genomes. *Journal of Molecular Biology*, *305*(3), 567–580.

Kwon, T., Sparks, J. A., Liao, F., & Blancaflor, E. B. (2018). ERULUS Is a Plasma Membrane-Localized Receptor-Like Kinase That Specifies Root Hair Growth by Maintaining Tip-Focused Cytoplasmic Calcium Oscillations. *The Plant Cell*, *30*(6), 1173–1177.

Kwon, T., Sparks, J. A., Nakashima, J., Allen, S. N., Tang, Y., & Blancaflor, E. B. (2015). Transcriptional response of Arabidopsis seedlings during spaceflight reveals peroxidase and cell wall remodeling genes associated with root hair development. *American Journal of Botany*, *102*(1), 21–35.

Lee, J.-Y., Colinas, J., Wang, J. Y., Mace, D., Ohler, U., & Benfey, P. N. (2006). Transcriptional and posttranscriptional regulation of transcription factor expression in Arabidopsis roots. *Proceedings of the National Academy of Sciences of the United States of America*, *103*(15), 6055–6060.

Masucci, J. D., & Schiefelbein, J. W. (1994). Root-Hair Initiation through an Auxin- and Ethylene-Associated Process'. *Plant Physiology*, *106*, 1335–1346.

Masucci, J. D., & Schiefelbein, J. W. (1994). The rhd6 Mutation of Arabidopsis thaliana Alters Root-Hair Initiation through an Auxin- and Ethylene-Associated Process. *Plant Physiology*, *106*(4), 1335–1346.

Masucci, J. D., & Schiefelbein, J. W. (1996). Hormones act downstream of TTG and GL2 to promote root hair outgrowth during epidermis development in the Arabidopsis root. *The Plant Cell*, *8*(9), 1505–1517.

Mendrinna, A., & Persson, S. (2015). Root hair growth: it's a one way street. *F1000prime Reports*, *7*, 23.

Möller, S., Croning, M. D., & Apweiler, R. (2001). Evaluation of methods for the prediction of membrane spanning regions. *Bioinformatics* , *17*(7), 646–653.

Ringli, C., Baumberger, N., Diet, A., Frey, B., & Keller, B. (2002). ACTIN2 is essential for bulge site selection and tip growth during root hair development of Arabidopsis. *Plant Physiology*, *129*(4), 1464–1472.

Schiefelbein, J. W., & Somerville, C. (1990). Genetic Control of Root Hair Development in Arabidopsis thaliana. *The Plant Cell*, *2*(3), 235–243.

Schoenaers, S., Balcerowicz, D., Breen, G., Hill, K., Zdanio, M., Mouille, G., Holman, T. J., Oh, J., Wilson, M. H., Nikonorova, N., Vu, L. D., De Smet, I., Swarup, R., De Vos, W. H., Pintelon, I., Adriaensen, D., Grierson, C., Bennett, M. J., & Vissenberg, K. (2018). The Auxin-Regulated CrRLK1L Kinase ERULUS Controls Cell Wall Composition during Root Hair Tip Growth. *Current Biology: CB*, *28*(5), 722–732.e6.

Shiu, S. H., & Bleecker, A. B. (2001). Receptor-like kinases from Arabidopsis form a monophyletic gene family related to animal receptor kinases. *Proceedings of the National Academy of Sciences of the United States of America*, *98*(19), 10763–10768.

Shiu, S. H., & Bleecker, A. B. (2003). Expansion of the receptor-like kinase/Pelle gene family and receptor-like proteins in Arabidopsis. *Plant Physiology*, *132*(2), 530–543.

Singh, S. K., Fischer, U., Singh, M., Grebe, M., & Marchant, A. (2008). Insight into the early steps of root hair formation revealed by the procuste1 cellulose synthase mutant of Arabidopsis thaliana. *BMC Plant Biology*, *8*, 57.

Sonnhammer, E. L., von Heijne, G., & Krogh, A. (1998). A hidden Markov model for predicting transmembrane helices in protein sequences. *Proceedings / ... International Conference on Intelligent Systems for Molecular Biology ; ISMB. International Conference on Intelligent Systems for Molecular Biology*, *6*, 175–182.

Szklarczyk, D., Gable, A. L., Lyon, D., Junge, A., Wyder, S., Huerta-Cepas, J., Simonovic, M., Doncheva, N. T., Morris, J. H., Bork, P., Jensen, L. J., & Mering, C. von. (2019). STRING v11: protein–protein association networks with increased coverage, supporting functional discovery in genome-wide experimental datasets. *Nucleic Acids Research*, *47*(D1), D607–D613.

Van Norman, J. M., Zhang, J., Cazzonelli, C. I., Pogson, B. J., Harrison, P. J., Bugg, T. D. H., Chan, K. X., Thompson, A. J., & Benfey, P. N. (2014). Periodic root branching in Arabidopsis requires synthesis of an uncharacterized carotenoid derivative. *Proceedings of the National Academy of Sciences of the United States of America*, *111*(13), E1300–E1309.

CHAPTER FOUR: DISCUSSION AND FUTURE DIRECTIONS

The work presented here used primarily *in-vivo* techniques and live-cell imaging using *Arabidopsis* roots to understand the mechanisms that govern WFL polar localization and how WFL polarity is linked to its biological function in root hair (RH) positioning. To more completely understand WFL polarity, it will be necessary to investigate potential polar protein partners that may facilitate WFL polar localization to distinct plasma membrane domains. Furthermore, to determine the intricacies of WFL function in root development, it will be important to examine the function of other LRR-RLKs that are closely related to WFL. These experiments can provide information about the underlying mechanisms of WFL localization and how WFL contributes to RH positioning.

Establishment and maintenance of WFL polar localization at the plasma membrane

Endomembrane protein trafficking is closely related to the establishment and maintenance of PM protein polarity (Muroyama & Bergmann, 2019; Raggi et al., 2020; Rodriguez-Furlan et al., 2019). Our results indicate that WFL polarity at the PM is primarily maintained by constant secretion and degradation. The WFL biosynthetic secretory traffic is directed through a BFA sensitive pathway, however, BFA interference with protein delivery does not alter WFL polarity as it has been described for PIN1 (Tanaka et al., 2014). Additionally, endocytosis and

recycling does not appear to be responsible for maintaining the pool of WFL at the PM, which instead relies mainly on *de novo* protein synthesis. Therefore, WFL polar secretion appears to be similar to that of other laterally localized proteins, such as POLAR AUXIN TRANSPORT INHIBITOR-SENSITIVE 1/PLEIOTROPIC DRUG RESISTANCE 9 (PIS1/PDR9/ABCG37) (Langowski et al., 2010; Łangowski et al., 2016).

We observe that full length WFL localizes to the same polar domain regardless of cell identity, suggesting that, similar to what has been proposed for some nutrient transporters (Alassimone et al., 2010), polar localization of full length WFL may be directed by a cue originating from the stele. However, not all proteins with lateral polar localization are dependent upon a cue that originates from the inner cell layers of the root. Accordingly, polar localization of IRK is informed locally by adjacent cells and changes depending on cell type (Campos et al., 2020). Thus, it is clear that there are multiple ways that cells interpret and respond to positional information for polar protein localization.

Despite our hypothesis that localization of full length WFL is informed by organ-level polarity cues, removal of the intracellular domains indicates that a cue from the stele is not sufficient to localize truncated WFL. WFL∆JxK-GFP reveals differential localization depending on cell identity and developmental context. WFL∆JxK-GFP localizes to the outer polar domain of epidermal cells and the

immature cortex cells, whereas in mature cortex cells, WFL∆JxK-GFP is also sometimes present at the inner PM domain. Strikingly, WFL∆JxK-GFP cannot be detected in endodermal cells of the primary root, but in lateral roots, exhibits nonpolar localization in the endodermis. Therefore, it is possible that when the intracellular domains are absent, the protein is redirected to different secretion pathways in different cell types. This hypothesis is consistent with the existence of multiple endomembrane trafficking pathways governing polar localization of transmembrane receptors in plants (Li et al., 2017). These results underscore the necessity of WFL intracellular domains to direct its polar localization, which is informed by context specific factors that take into account cell type and developmental stage.

Full length WFL localizes to the inner polar domain of root epidermal cells and to a specialized portion of the outer polar domain of hair cells called the root hair initiation domain (RHID). Dual lateral polar localization like we observe for WFL has not been previously reported for any other polarized protein, making it an intriguing subject for the study of cell polarity. Additionally, upon removal of the WFL intracellular domains, we observe that WFL∆JxK-GFP is mislocalized to the outer polar domain. This mislocalization of WFL∆JxK-GFP emphasizes the importance of the intracellular domains for normal WFL localization, and suggests that these domains may be important for polar localization of other LRR-RLKs. Similar to WFL, removal of the cytoplasmic domains of KINASE ON

THE INNERSIDE (KOIN) results in nonpolar localization in root endodermal cells. In contrast, removal of the intracellular domains of INFLORESCENCE AND ROOT APICES RECEPTOR KINASE (IRK), does not affect its polar localization (Rodriguez-Furlán et al. 2021). The different localization outcomes for these three truncated versions of polarized receptors highlights the diversity by which polar localization is achieved among LRR-RLKs.

In addition to mislocalization to the outer polar polar domain, it is notable that in H cells, WFL∆JxK-GFP is specifically excluded from the RHIDs and RH bulges, suggesting that secretion and localization at the plasma membrane of both the full length and truncated versions of WFL are subject to strict regulation. It is unclear how the inverse localization pattern of full-length and truncated WFL is achieved, but the possibilities include interaction, or lack thereof, with another polar protein partner. In support of this, recruitment of RHO-RELATED PROTEIN FROM PLANTS 2 (ROP2) to the RHID requires the initial polar localization of GUANINE NUCLEOTIDE EXCHANGE FACTOR3 (GEF3) to this site (Denninger et al., 2019). Therefore, it is possible that in the absence of its intracellular domains, WFL∆JxK-GFP is unable to interact with the binding partner that is driving WFL polar localization to the inner polar domains and the RHID/RH bulges. However, this explanation is not very satisfying as it implies that without its correct binding partner, WFL would have a reciprocal localization pattern in H cells (identical to WFL∆JxK-GFP) or that truncated WFL interacts with a different

protein that happens to have the opposite localization. Further research will be necessary to identify WFL binding partners and determine whether they influence WFL polarity.

WFL functions in RH positioning

To understand the function of WFL in root development, we generated a putative null allele, *wfl-1*. However, we were unable to identify an abnormal phenotype in *wfl-1*. WFL belongs to the receptor-like kinase (RLK) gene family, the largest gene family in Arabidopsis with over 600 members. Within the RLK family, there are over 200 LRR-RLKs that are predicted to be functionally redundant (Diévart & Clark, 2003, 2004). Therefore, in the absence of WFL, it is possible that another receptor that is closely related to WFL may be sufficient for normal function. We identified four of these receptors and initiated the production of the double mutants with *wfl-1*. Future phenotypic analyses using double and triple mutants will be necessary to determine the functional significance of WFL in root development.

Although we did not detect an abnormal phenotype in *wfl-1* roots, we found that upon overexpression of WFL, RH position is shifted toward the rootward edge of H cells. Polarized protein localization involved in intracellular signaling has been shown to be linked to function. In the meristematic zone, IRK is localized to the outer polar domain of root endodermal cells and *irk* mutants have altered cell

divisions in that cell type (Campos et al., 2020). Additionally, in the differentiation zone, SCHENGEN1 (SGN1), a receptor-like cytoplasmic kinase and SGN3/GASSHO1, an LRR-RLK, are polarly localized in maturing root endodermal cells and required for Casparian strip formation (Alassimone et al., 2016; Pfister et al., 2014). Therefore, WFL polar localization to RHIDs and RH bulges is consistent with a potential role in WFL in RH positioning.

To link WFL to known factors in RH positioning, we examined a transcriptomic dataset that identified a core set of RHD6-dependent genes involved in root epidermal cell differentiation (Bruex et al., 2012). RHD6 is a bHLH transcription factor and RHs in *rhd6* mutants are also shifted toward the rootward edge of H cells (Masucci & Schiefelbein, 1994), however *WFL* was not among the core set of RHD6-dependent genes. This suggests *WFL* is not a direct downstream target of RHD6 and may operate in a separate pathway or may regulate another integral component of RH positioning.

In addition to the RHIDs and RH bulges, WFL polarly localizes to the outermost layers of the lateral root cap (LRC) and other cell types in the elongation and differentiation zones, all of which are areas of the root where dramatic changes to the cell wall are taking place. Roots overexpressing WFL-GFP appear to be more sensitive to mechanical stress as they are frequently damaged during routine confocal imaging, but this sensitivity can be alleviated by exposure to -Pi

growth conditions. This phenotype and the presence of WFL at these positions of cell wall modification together with a shifted RH position upon WFL overexpression make it very tempting to speculate that WFL is involved in cell wall modification or integrity.

A key component of plant cell walls is cellulose, which provides structural integrity to the plant body and is the main load-bearing component of the cell wall (Cosgrove, 2005). Similar to WFL-GFP, RH position is shifted toward the rootward edge of H cells of *procuste1* mutants, which have a defect in CELLULOSE SYNTHASE6 (CESA6), indicating that cellulose is also important for normal RH positioning (Singh et al., 2008). To investigate cellulose composition in WFL-GFP roots, we treated them with isoxaben, but did not observe any differences between WFL-GFP and WT. The cell wall is structurally complex, and while these results suggest that WFL-GFP roots do not have a defect in cellulose biosynthesis, WFL may regulate another cell wall component.

Recently, FERONIA (FER), another LRR-RLK, was shown to interact with cell wall-associated protein, LEUCINE-RICH REPEAT/EXTENSIN 1 (LRX1), to coordinate cell wall loosening during vacuolar expansion (Dünser et al., 2019). Interestingly, the Search Tool for the Retrieval of Interacting Genes/Proteins (STRING) database predicts that WFL interacts with a RH-specific proline-rich extensin-like family protein (EXT15, AT1G23720) (Szklarczyk et al., 2019).

Extensins are structural proteins that act as a scaffolding network and may serve as a template for assembly of the pectin matrix of the cell wall (Baumberger et al., 2003; Lamport et al., 2011). WFL is also predicted to interact with two RH-specific Class III (CIII) peroxidase (PRX) proteins (PRX27, AT3G01190 and PRX57, AT5G17820), and it has been proposed that pectin may facilitate interactions between PRXs and EXTs (Passardi et al., 2005). Further research into a possible role for WFL in cell wall modification through these cell wall-associated proteins and their potential interaction with WFL are intriguing areas for future study.

Additionally, we observed that sensitivity to mechanical stress can be overcome by maintaining stable osmotic conditions. During RH development, the main driver of expansion at the RH tip is turgor pressure, and coordination of turgor pressure with the growing cell wall is critical to accommodate the expanding cell (Grierson et al., 2014; Mendrinna & Persson, 2015). Turgor pressure is regulated by sensing changes in osmolarity, not internal pressure (Lew, 1996). We examined if WFL had a role in modulating turgor pressure by examining the sensitivity of different genotypes to plasmolysis. We found that roots expressing WFL-GFP and WT responded similarly to plasmolysis. However, WFLΔJxK-GFP roots appear to be less sensitive to plasmolysis. Furthermore, RH position is normal in WFLΔJxK-GFP roots, indicating that WFL intracellular domains are important to inform RH position. These results begin to link WFL proteins to

function in RH positioning and the modulation of turgor pressure. Furthermore they suggest that WFL intracellular domains may be important for sensing osmotic changes and/or communicating this information throughout the cell during RH development.

Our observations demonstrate that WFL is a polarly localized LRR-RLK with unique localization in H cells that is linked to its function in RH positioning. The importance of the WFL intracellular domains is highlighted by the change in WFL localization from the inner to the outer polar domain, upon their removal. This is further underscored by the exclusion of WFLΔJxK-GFP from RHIDs and bulges. Our results suggest that polar localization of WFL is subject to precise spatiotemporal regulation. It is also clear that WFL intracellular domains are functionally important for RH positioning, as only overexpression of the full length protein results in a shift in RH position and truncated WFL is less sensitive to osmotic conditions that induce plasmolysis. We propose that the specific polar localization of WFL is linked to WFL function to modulate developmental events in the root's longitudinal axis that require changes in the cell wall.

The identification of receptor kinases with polar localization provides a new set of conceptual and molecular tools to investigate cell polarity in plants. Unlike transporters, polar localization of receptor proteins is not implicitly tied to their molecular function, suggesting that establishment of polarized signaling domains

to perceive extracellular cues is functionally important. There is a long-standing hypothesis that directional signaling and positional information are key drivers of plant development and the identification of polarized receptor kinases, like WFL, supports this hypothesis.

REFERENCES

Alassimone, J., Fujita, S., Doblas, V. G., van Dop, M., Barberon, M., Kalmbach, L., Vermeer, J. E. M., Rojas-Murcia, N., Santuari, L., Hardtke, C. S., & Geldner, N. (2016). Polarly localized kinase SGN1 is required for Casparian strip integrity and positioning. *Nature Plants, 2,* 16113.

Alassimone, J., Naseer, S., & Geldner, N. (2010). A developmental framework for endodermal differentiation and polarity. *Proceedings of the National Academy of Sciences of the United States of America*, *107*(11), 5214–5219.

Baumberger, N., Doesseger, B., Guyot, R., Diet, A., Parsons, R. L., Clark, M. A., Simmons, M. P., Bedinger, P., Goff, S. A., Ringli, C., & Keller, B. (2003). Whole-genome comparison of leucine-rich repeat extensins in Arabidopsis and rice. A conserved family of cell wall proteins form a vegetative and a reproductive clade. *Plant Physiology*, *131*(3), 1313–1326.

Bruex, A., Kainkaryam, R. M., Wieckowski, Y., Kang, Y. H., Bernhardt, C., Xia, Y., Zheng, X., Wang, J. Y., Lee, M. M., Benfey, P., Woolf, P. J., & Schiefelbein, J. (2012). A gene regulatory network for root epidermis cell differentiation in Arabidopsis. *PLoS Genetics*, *8*(1), e1002446.

Campos, R., Goff, J., Rodriguez-Furlan, C., & Van Norman, J. M. (2020). The Arabidopsis Receptor Kinase IRK Is Polarized and Represses Specific Cell Divisions in Roots. *Developmental Cell*, *52*(2), 183–195.e4.

Cosgrove, D. J. (2005). Growth of the plant cell wall. *Nature Reviews. Molecular Cell Biology*, *6*(11), 850–861.

Denninger, P., Reichelt, A., Schmidt, V. A. F., Mehlhorn, D. G., Asseck, L. Y., Stanley, C. E., Keinath, N. F., Evers, J.-F., Grefen, C., & Grossmann, G. (2019). Distinct RopGEFs Successively Drive Polarization and Outgrowth of Root Hairs. *Current Biology: CB*, *29*(11), 1854–1865.e5.

Diévart, A., & Clark, S. E. (2003). Using mutant alleles to determine the structure and function of leucine-rich repeat receptor-like kinases. *Current Opinion in Plant Biology*, *6*(5), 507–516.

Diévart, A., & Clark, S. E. (2004). LRR-containing receptors regulating plant development and defense. *Development* , *131*(2), 251–261.

Dünser, K., Gupta, S., Herger, A., Feraru, M. I., Ringli, C., & Kleine-Vehn, J. (2019). Extracellular matrix sensing by FERONIA and Leucine-Rich Repeat Extensins controls vacuolar expansion during cellular elongation in Arabidopsis thaliana. *The EMBO Journal*, *38*(7). https://doi.org/10.15252/embj.2018100353

Grierson, C., Nielsen, E., Ketelaarc, T., & Schiefelbein, J. (2014). Root hairs. *The Arabidopsis Book / American Society of Plant Biologists*, *12*, e0172.

Lamport, D. T. A., Kieliszewski, M. J., Chen, Y., & Cannon, M. C. (2011). Role of the extensin superfamily in primary cell wall architecture. *Plant Physiology*, *156*(1), 11–19.

Langowski, L., Růzicka, K., Naramoto, S., Kleine-Vehn, J., & Friml, J. (2010). Trafficking to the outer polar domain defines the root-soil interface. *Current Biology: CB*, *20*(10), 904–908.

Łangowski, Ł., Wabnik, K., Li, H., Vanneste, S., Naramoto, S., Tanaka, H., & Friml, J. (2016). Cellular mechanisms for cargo delivery and polarity maintenance at different polar domains in plant cells. *Cell Discovery*, *2*, 16018.

Lew, R. R. (1996). Pressure regulation of the electrical properties of growing Arabidopsis thaliana L. root hairs. *Plant Physiology*, *112*(3), 1089–1100.

Li, R., Rodriguez-Furlan, C., Wang, J., van de Ven, W., Gao, T., Raikhel, N. V., & Hicks, G. R. (2017). Different Endomembrane Trafficking Pathways Establish Apical and Basal Polarities. *The Plant Cell*, *29*(1), 90–108.

Masucci, J. D., & Schiefelbein, J. W. (1994). The rhd6 Mutation of Arabidopsis thaliana Alters Root-Hair Initiation through an Auxin- and Ethylene-Associated Process. *Plant Physiology*, *106*(4), 1335–1346.

Mendrinna, A., & Persson, S. (2015). Root hair growth: it's a one way street. *F1000prime Reports*, *7*, 23.

Muroyama, A., & Bergmann, D. (2019). Plant Cell Polarity: Creating Diversity from Inside the Box. *Annual Review of Cell and Developmental Biology*, *35*, 309–336.

Passardi, F., Cosio, C., Penel, C., & Dunand, C. (2005). Peroxidases have more functions than a Swiss army knife. *Plant Cell Reports*, *24*(5), 255–265.

Pfister, A., Barberon, M., Alassimone, J., Kalmbach, L., Lee, Y., Vermeer, J. E. M., Yamazaki, M., Li, G., Maurel, C., Takano, J., Kamiya, T., Salt, D. E., Roppolo, D., & Geldner, N. (2014). A receptor-like kinase mutant with absent endodermal diffusion barrier displays selective nutrient homeostasis defects. *eLife*, *3*, e03115.

Raggi, S., Demes, E., Liu, S., Verger, S., & Robert, S. (2020). Polar expedition: mechanisms for protein polar localization. *Current Opinion in Plant Biology*, *53*, 134–140.

Rodriguez-Furlan, C., Minina, E. A., & Hicks, G. R. (2019). Remove, Recycle, Degrade: Regulating Plasma Membrane Protein Accumulation. *The Plant Cell*, *31*(12), 2833–2854.

Singh, S. K., Fischer, U., Singh, M., Grebe, M., & Marchant, A. (2008). Insight into the early steps of root hair formation revealed by the procuste1 cellulose synthase mutant of Arabidopsis thaliana. *BMC Plant Biology*, *8*, 57.

Szklarczyk, D., Gable, A. L., Lyon, D., Junge, A., Wyder, S., Huerta-Cepas, J., Simonovic, M., Doncheva, N. T., Morris, J. H., Bork, P., Jensen, L. J., & Mering, C. von. (2019). STRING v11: protein–protein association networks with increased coverage, supporting functional discovery in genome-wide experimental datasets. *Nucleic Acids Research*, *47*(D1), D607–D613.

Tanaka, H., Nodzyłski, T., Kitakura, S., Feraru, M. I., Sasabe, M., Ishikawa, T., Kleine-Vehn, J., Kakimoto, T., & Friml, J. (2014). BEX1/ARF1A1C is required for BFA-sensitive recycling of PIN auxin transporters and auxin-mediated development in Arabidopsis. *Plant & Cell Physiology*, *55*(4), 737–749.